Volume 3 | Number 1 | January 2016

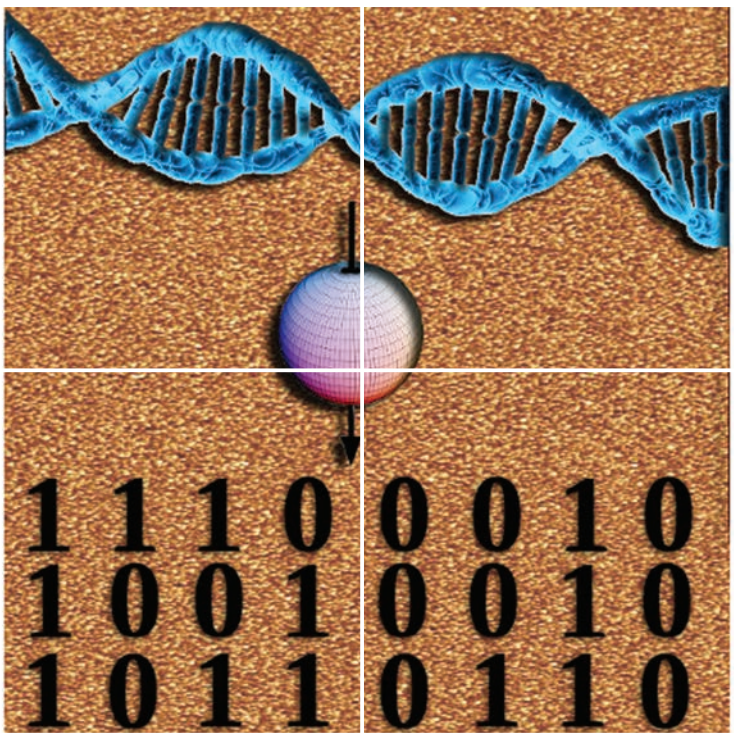

INORGANIC CHEMISTRY

FRONTIERS

Chinese Chemical Society
PEKING UNIVERSITY 1898
ROYAL SOCIETY OF CHEMISTRY

http://rsc.li/frontiers-inorganic

INORGANIC CHEMISTRY
FRONTIERS

REVIEW

Cite this: *Inorg. Chem. Front.*, 2016, **3**, 41

Nanozymes in bionanotechnology: from sensing to therapeutics and beyond†

Xiaoyu Wang,[a] Yihui Hu[a] and Hui Wei*[a,b]

Received 5th November 2015,
Accepted 5th December 2015

DOI: 10.1039/c5qi00240k

rsc.li/frontiers-inorganic

In the past few decades, researchers have developed lots of artificial enzymes with various materials to mimic the structures and functions of natural enzymes. Recently, nanozymes, nanomaterials with enzyme-like characteristics, are emerging as novel artificial enzymes, and attracting researchers' enormous interest. Remarkable advances have been made in the area of nanozymes due to their unique properties compared with natural enzymes and classic artificial enzymes. Until now, lots of nanomaterials have been studied to mimic various natural enzymes for wide applications. To highlight the recent progress of nanozymes (especially in bionanotechnology), here we discuss the diverse applications of nanozymes, which range from sensing, imaging, and therapeutics, to logic gates, pollutant removal, water treatment, *etc*. Finally, we address the current challenges facing nanozyme research as well as possible directions to fulfill their great potential in future.

1. Introduction

Nanozymes are nanomaterials with enzyme-like characteristics.[1] As an emerging research area in the field of artificial enzymes, nanozymes have attracted researchers' enormous interest due to their unique properties compared with natural enzymes and classic artificial enzymes.[1–4] Compared with natural enzymes, nanozymes are advantageous in several aspects, such as low cost, ease of mass production, robustness to harsh environments, high stability, long-term storage, and size/composition dependent activity.[1] Besides, nanozymes have also shown unique properties compared with other artificial enzymes in terms of their size- (shape-, structure-, composition-) dependent catalytic activities, integrated (multi-)functions besides catalysis, large surface area for further modification and bioconjugation, smart response to external stimuli, self-assembly capability, *etc*.[1] Until now, lots of nanomaterials have been explored to mimic various natural enzymes, such as catalase, oxidase, peroxidase, superoxide dismutase (SOD), esterase, nuclease, phosphatase, protease and ferroxidase (Fig. 1).[5–26] These nanozymes have been extensively investigated for diverse applications in bionanotechnology, ranging from biosensing and bioimaging to tissue engineering, therapeutics and beyond. In 2013, we have made a comprehensive review on nanozymes.[1] Since then, substantial progress has been achieved in the field. To highlight the recent exciting progress, the present review discusses the key reports of nanozymes, especially their applications in bionanotechnology. A few early studies are also included to provide a historic view of nanozyme research. Several well established mechanisms about nanozyme catalytic reactions are also covered. The current challenges facing nanozyme research as well as possible directions to fulfill their great potential are discussed in the final section.

[a]*Department of Biomedical Engineering, College of Engineering and Applied Sciences, Collaborative Innovation Center of Chemistry for Life Sciences, Nanjing National Laboratory of Microstructures, Nanjing University, Nanjing 210093, China. E-mail: weihui@nju.edu.cn; http://weilab.nju.edu.cn; Fax: +86-25-83594648; Tel: +86-25-83593272*

[b]*State Key Laboratory of Electroanalytical Chemistry, Changchun Institute of Applied Chemistry, Chinese Academy of Sciences, Changchun, Jilin 130022, China*

†Electronic supplementary information (ESI) available: Supplementary tables. See DOI: 10.1039/c5qi00240k

Hui Wei

Hui Wei received his B.S. degree from Nanjing University in 2003 and PhD degree from the Changchun Institute of Applied Chemistry, Chinese Academy of Sciences in 2008. Currently he is a professor at Nanjing University, working on the design and synthesis of functional nanomaterials (such as nanozymes) and the development of new methodologies for analytical and biomedical applications. He is an Editorial Board Member for Scientific Reports.

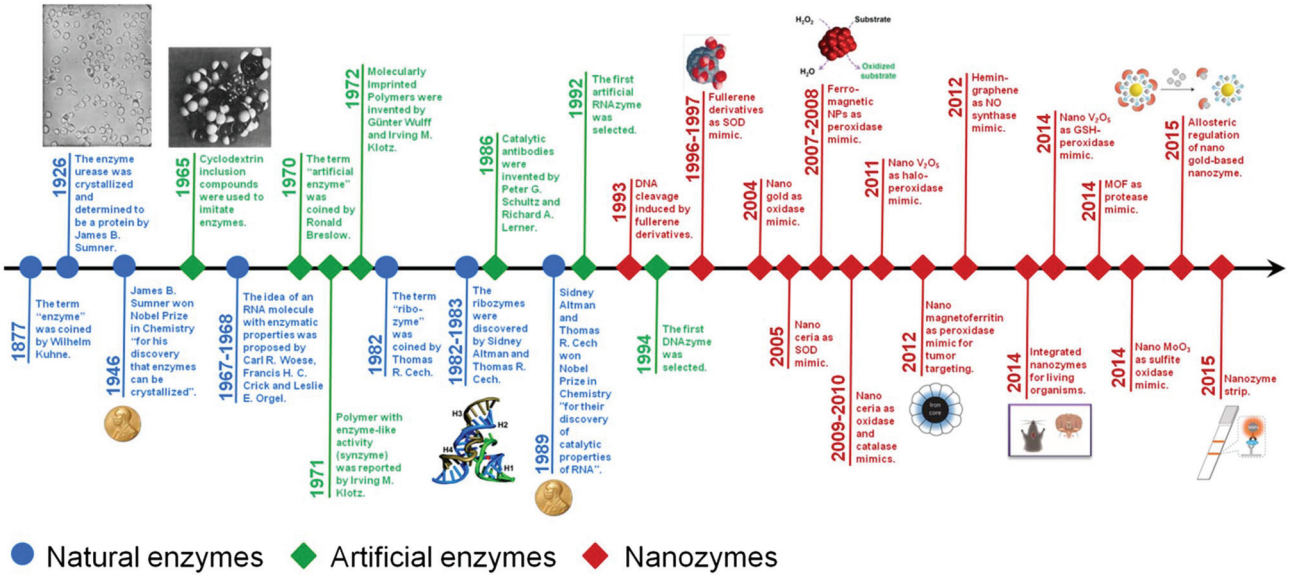

Fig. 1 A brief timeline for the development of artificial enzymes (natural enzymes are also listed for comparison) (see Table S1, ESI† for related references). Adapted with permission from ref. 1. Copyright (2013) Royal Society of Chemistry.

We do not attempt to cover all the related publications on nanozymes due to space limitations. Readers are referred to numerous critical reviews and the references therein for more information.[1–4,27–36]

2. Nanozymes for sensing and imaging

Since the seminal reports by Yan's and Wang's groups,[11,12] nanozymes have been widely used for detecting a variety of important targets, such as bioactive small molecules, metal ions, nucleic acids, cancer cells and even bacteria.

2.1 Nanozymes for H_2O_2 sensing

H_2O_2 detection is of great interest owing to its important roles in biology, medicine, food industry and environmental protection.[37,38] H_2O_2 detection is usually achieved by using nanomaterials' peroxidase mimicking activities, in which the H_2O_2-mediated oxidation of a substrate is catalyzed by a peroxidase mimic (Scheme 1 and Fig. 2). By monitoring the production of the oxidized substrate (*i.e.*, A in Scheme 1), H_2O_2 can be determined.

Wei and Wang have developed a colorimetric method for H_2O_2 detection.[12] They used Fe_3O_4 magnetic nanoparticles (MNPs) as the peroxidase mimic and ABTS as the substrate for signalling (Fig. 2a). The presence of H_2O_2 generated green coloured $ABTS^{\bullet+}$, which could be quantified by absorption

$$AH_2 + ROOH \xrightarrow{\text{Peroxidase}} A + ROH + H_2O \quad (1)$$

Scheme 1 The reaction catalyzed by peroxidase.

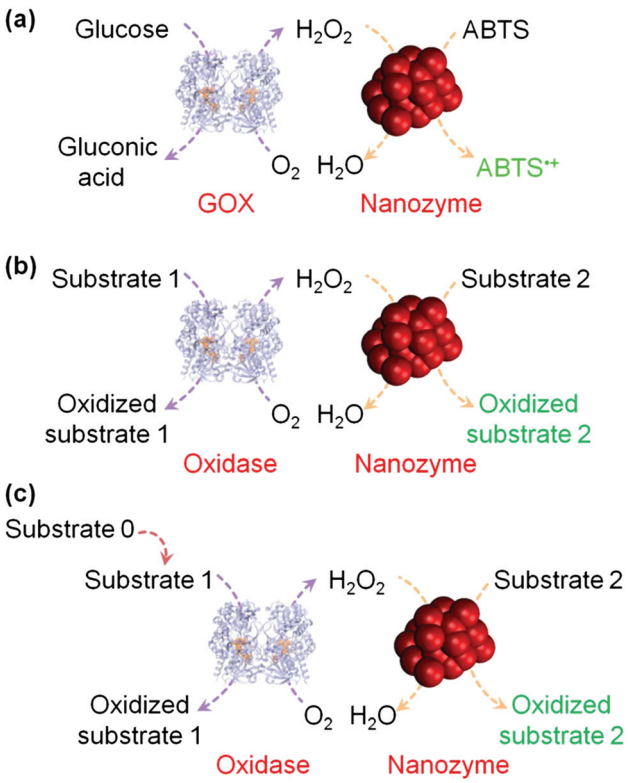

Fig. 2 (a) Nanozyme as peroxidase mimic for colorimetric sensing of H_2O_2, and glucose when combined with glucose oxidase. (b) The sensing format in (a) could be extended to other targets (substrate 1 here) when combined with a suitable oxidase. (c) Target of interest as substrate 0 could be determined if it could be converted into an oxidase substrate. Numerous transduction signals can be adopted for sensing (such as colorimetric, fluorometric, chemiluminescent, and SERS signals when the corresponding substrates are used; and electrochemical signals when a nanozyme is immobilized on an electrode). Adapted with permission from ref. 1. Copyright (2013) Royal Society of Chemistry.

spectra or even visualized by the naked eye. Since then, considerable amount of studies have been devoted to H_2O_2 detection by exploring various nanomaterials' peroxidase mimicking activities (also see Table S2, ESI†).[39–86] Besides colorimetric detection with peroxidase substrates (such as ABTS, 4-AAP, DPD, OPD, and TMB), H_2O_2 has also been determined *via* fluorescent, electrochemical and surface enhanced Raman scattering (SERS) methods.[42,52,56,58,64,68,72,73,77,79,82,84]

Recently, Zhang and co-workers developed 3D Fe- and N-doped carbon nanostructures to mimic peroxidase.[52] Due to the presence of highly active Fe–N and doped-N species as well as the large surface area, the nanostructures exhibited good peroxidase mimicking activity. They further constructed a fluorescent sensor for H_2O_2 detection with the developed nanozyme, which had a linear range from 100 nM to 100 μM and a detection limit of 68 nM. In another study, Fe_7S_8 nanowires with intrinsic peroxidase-like activity have been studied for fluorescent detection of H_2O_2.[59]

Fang *et al.* used Fe_3O_4/reduced graphene oxide (rGO) nanocomposites as the peroxidase mimic to prepare the modified glassy carbon electrode for electrochemical sensing of H_2O_2 (Fig. 3).[67] The developed electrochemical sensor showed good selectivity toward H_2O_2 detection over several metal ions (Na^+, K^+, Ag^+, Mg^{2+}, and Cu^{2+}) and bioactive small molecules (glutathione (GSH), glucose, ascorbic acid, L-cysteine, and uric acid). Interestingly, with the developed electrochemical biosensor, they were able to monitor CdTe quantum dot-stimulated extracellular H_2O_2 release from living HeLa cells. This study may be useful for understanding the biological effects of nanomaterials.

When a target of interest is used as the substrate for the peroxidase, it can be measured with nanozymes as peroxidase mimics. 5-Hydroxyindole-3-acetic acid (5-HIAA), an indoleamine metabolite, is an important diagnostic biomarker for carcinoid tumours. To selectively oxidize 5-HIAA with hemin as a peroxidase mimic, magnetic molecularly imprinted catalytic polymers were fabricated.[87] The products of 5-HIAA oxidation were then separated and detected with HPLC to quantitatively measure 5-HIAA.

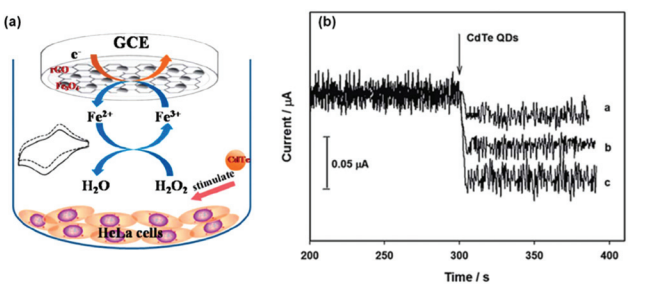

Fig. 3 Electrochemical monitoring of H_2O_2 release from living cells stimulated by CdTe quantum dots with a nanozyme-modified electrode. Reprinted with permission from ref. 67. Copyright (2014) Royal Society of Chemistry.

2.2 Nanozymes for glucose (and other oxidase substrate) sensing

As shown in Fig. 2, when an oxidase is combined with a peroxidase mimic, the corresponding oxidase substrate can be determined. By combining glucose oxidase with Fe_3O_4 MNPs as the peroxidase mimic, a sensitive and selective colorimetric approach to glucose detection was reported by Wei *et al.* (Fig. 4).[12]

Until now, varieties of nanozymes with peroxidase activities have been developed and used for glucose detection when they were combined with glucose oxidase (also see Table S3, ESI†).[39–44,46–52,59–65,69–71,78,88–121] For example, NiTe thorny nanostructures have been synthesized and used for sensitive and selective glucose detection by Wan *et al.*[105] Some of the nanozymes have already been successfully used for determining glucose in drinks and biological samples (such as blood and urine).[89,94,104,106,108,112]

To further promote cascade reactions, glucose oxidase and a nanozyme could be assembled together as integrated nanocomposites.[118,119] Qu *et al.* recently reported an inspiring method for glucose detection.[104] They replaced both glucose oxidase and peroxidase with the nanomaterial mimics (*i.e.*, gold nanoparticles (AuNPs) as the glucose oxidase mimic and V_2O_5 nanowires as the peroxidase mimic) (Fig. 5). The two nanozymes were assembled together *via* polymerized dopamine for cascade reactions. By eliminating the use of both natural enzymes, the current system displayed higher robustness but at much lower cost.

As indicated by Fig. 2b, when other oxidases are used, their corresponding substrates as targets of interest can be detected. Choline, D-alanine, lactate, uric acid, and xanthine have been determined with the strategy shown in Fig. 2b.[64,74,122–124] For example, when $NaYF_4$:Yb,Er nanoparticles as a peroxidase mimic was combined with uricase, uric acid has been determined.[124] The proposed method had good selectivity against

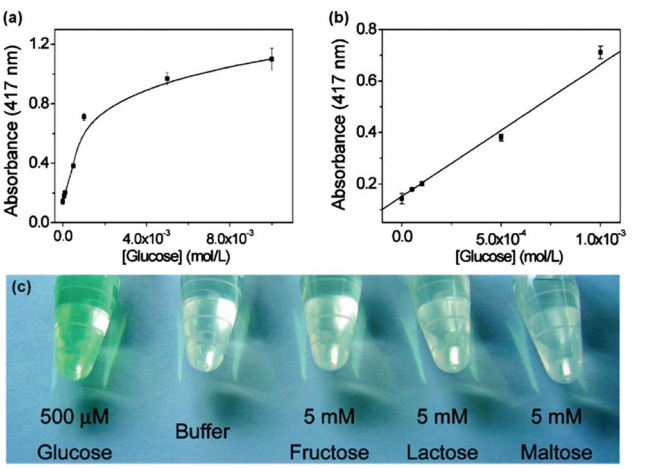

Fig. 4 Colorimetric detection of glucose by combining glucose oxidase with Fe_3O_4 MNPs as peroxidase mimic. Reprinted with permission from ref. 12. Copyright (2008) American Chemical Society.

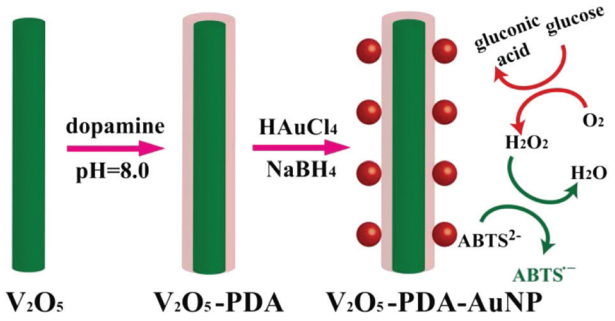

Fig. 5 Colorimetric detection of glucose by assembled AuNPs onto V_2O_5 nanowires as glucose oxidase and peroxidase mimics, respectively. Reprinted with permission from ref. 104. Copyright (2014) John Wiley and Sons.

several biomolecules, such as creatinine, ascorbic acid, glucose, cholesterol, triglyceride, and urea. Moreover, the uric acid in a clinical human serum sample was successfully measured *via* the developed method, which matched well with the established method.

Several studies also demonstrated that the targets of interest as substrate 0 could be determined if they could be converted into oxidase substrates (Fig. 2c).[123,125–127] Using acetylcholinesterase, choline oxidase and Au/Ag nanoparticles as the peroxidase mimic, Wang *et al.* reported the sensitive detection of acetylcholine.[125] With Wang's method, a detection limit of 0.21 nM was obtained. Based on the inhibition of acetylcholinesterase's activity with organophosphates, Liang and co-workers later developed a rapid and sensitive strategy for detecting organophosphorus pesticides and nerve agents (such as Sarin).[126]

2.3 Sensing targets of interest by modulating peroxidase mimics (or oxidase mimics) catalyzed reactions

As shown in Fig. 6, by modulating the peroxidase mimic catalyzed reactions, the targets of interest can be detected.[62,128–138] So far, these targets have already covered a wide range of molecules, such as ascorbic acid, biothiols (*e.g.*, cysteine), catechol, dopamine, melamine, phosphate, trypsin, *etc.*[62,128–138]

Fig. 6 By modulating the peroxidase mimics catalyzed reactions (*e.g.*, inhibiting the nanozymes' activity, consuming H_2O_2, or converting the coloured oxidized substrate to colourless product), the targets of interests can be detected.

By using C-rich DNA as the template, Sun *et al.* synthesized bimetallic Au_xPt_y and studied their peroxidase mimicking activities.[134] Their results revealed that the nanozymes' activities could be tuned by manipulating the ratios of $x:y$. After demonstrating the high peroxidase mimicking activity of the Au_2Pt_1 nanozyme, they then used it for detection of biothiols (*i.e.*, cysteine and homocysteine), which was based on the thiol-induced inhibition of the nanozyme's activities. The proposed strategy showed good selectivity against non-thiol-containing amino acids. Moreover, with Sun's sensing strategy, cysteine spiked in human serum was successfully detected with good recovery. Lin *et al.* suggested that the presence of cysteine not only inhibited the nanozyme's activities but also reduced the oxidized substrate (such as oxidized TMB).[135] Due to such a synergetic effect, a detection limit of 1.2 nM was obtained for cysteine detection. Ascorbic acid, one of the physiologically important neurochemicals,[139] was detected on the basis of its inhibition effect on CuNPs@C nanocomposites' peroxidase-like activity.[131] Several ions such as phosphate and uranyl ions have been detected based on their inhibition effects on peroxidase-like nanozymes.[136,137]

By reacting with and consuming H_2O_2, a number of bioactive small molecules (such as ascorbic acid, catechol, dopamine, GSH) have been detected.[62,130–133] For example, catechol in the Yellow river was determined using Fe_3O_4 MNPs as the peroxidase mimic.[132]

An innovative concept for the chemiluminescence detection of pesticides was reported.[140] The Fe_3O_4 MNPs as peroxidase mimics catalyzed the generation of chemiluminescence from luminol, which could be quenched by ethanol. However, the quenching was reversed when pesticides were bound onto Fe_3O_4 MNPs. By "turning on" the chemiluminescence of luminol, nonredox active pesticides were sensitively detected. More interestingly, Fe_3O_4 MNPs with different surface ligands exhibited unique chemiluminescence patterns towards different pesticides. Thus, simultaneous detection of pesticides could be achieved *via* the developed method.

Oxidase uses oxygen to oxidize its substrates (Scheme 2). Similar to natural oxidase, nanomaterial-based oxidase mimics have been used for sensing the corresponding substrates.[141–144] Hayat *et al.* evaluated the oxidase mimicking activity of nanoceria and developed a colorimetric assay for dopamine and catechol.[143] By carefully choosing the nanoceria

$$A_{red} + O_2 + H_2O \xrightarrow{\text{Oxidase}} A_{ox} + H_2O_2 \quad (2a)$$

$$A_{red} + O_2 \xrightarrow{\text{Oxidase}} A_{ox} + H_2O \quad (2b)$$

$$A_{red} + O_2 \xrightarrow{\text{Oxidase}} A_{ox} + O_2^{\bullet -} \quad (2c)$$

Scheme 2 The reactions catalyzed by oxidase.

type, buffer composition, pH, *etc*., they demonstrated good selectivity for dopamine and catechol detection with respect to several interferences.

Sulfite is an important additive in food and wine. It can tune the oxidase mimicking activity of $CoFe_2O_4$ nanoparticles. Zhang *et al.* discovered that sulfite at low concentration inhibited the oxidase mimicking activity of $CoFe_2O_4$ nanoparticles while a high concentration of sulfite exhibited enhancement effects.[141] On the basis of this phenomenon, they reported a chemiluminescent assay for sulfite determination in white wines. Sulfite in food was also measured by exploring its inhibition effect on the oxidase mimicking activity of Co_3O_4 nanoparticles.[142]

2.4 Nanozymes for nucleic acid sensing

Several strategies have been developed for nucleic acid detection using nanozymes.[104,145–155] The reported protocols can be roughly classified into two types. One type of assay uses nanozymes as alternative tags to classic dyes (or enzymes) to label the nucleic acid probe strand while the other type employs nucleic acids to tailor the nanozyme' activities.

For example, graphene-supported ferric porphyrin, acting as the peroxidase mimic, was bioconjugated onto streptavidin for electrochemically detecting the target DNA (Fig. 7a).[146] The hairpin DNA was immobilized onto a AuNP-modified electrode *via* Au–S interaction. In the presence of target DNA, the hairpin structure was opened and the pre-conjugated biotin was thus available for binding to the streptavidin–nanozyme conjugates. With the developed electrochemical sensor, as low as 22 aM of target DNA was detected. Thiramanas and coworkers reported the detection of bacterial DNA with Fe_3O_4 MNPs as peroxidase mimics *via* a sandwich assay.[147] The developed assay was used for monitoring bacteria in drinking and tap water.

Single-stranded DNA (ssDNA) and double-stranded DNA (dsDNA) exhibit different affinities towards several nanozymes. By modulating the peroxidase mimicking activity of AuNP/graphene hybrids with ssDNA and dsDNA, Liu *et al.* reported a colorimetric method for DNA detection (Fig. 7b).[156]

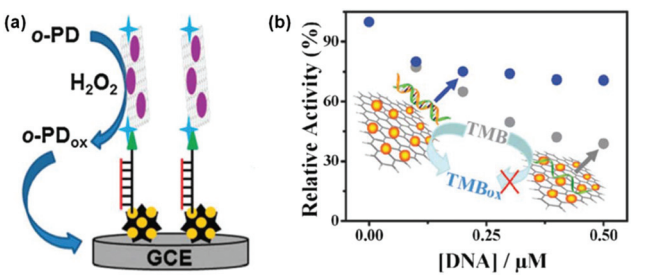

Fig. 7 Nucleic acid detection with nanozymes. (a) Electrochemical detection of DNA with graphene-supported ferric porphyrin as a peroxidase mimic. (b) DNA detection based on modulating the peroxidase mimicking activity of AuNP/graphene hybrids with ssDNA and dsDNA. (a) Reprinted with permission from ref. 146. Copyright (2013) Royal Society of Chemistry. (b) Reprinted with permission from ref. 156. Copyright (2012) Royal Society of Chemistry.

Despite the current progress, no RNA detection with nanozymes has been reported. Future efforts should also be focused on RNA detection, which is critical for disease diagnostics, *etc*.

Interestingly, while some reports showed that DNA could enhance the activity of several nanozymes,[157,158] others demonstrated that DNA could also inhibit the activity of certain nanozymes.[156,159,160] Liu *et al.* suggested that the enhanced activity of Fe_3O_4- and nanoceria-based peroxidase mimics by DNA was attributed to (i) the electrostatic interactions between the positively charged substrate TMB and the negatively charged phosphate backbone and (ii) the aromatic stacking between the DNA bases and TMB.[158] On the other hand, the much stronger binding between ssDNA and the gold nanoparticle-based nanozyme could completely prevent the interaction between the nanozyme and the substrate (even for positively-charged TMB), therefore inhibition effects were observed.[156,159] However, since the enhancing/inhibiting effects of DNA on the nanozyme' activity depend on many factors (such as the nature of nanozymes, the substrates, the DNA sequence, structures, *etc.*), more systematic studies are needed to understand the mechanisms involved.[161]

2.5 Nanozymes for aptasensors

Aptamers are selected short nucleic acid sequences, which are capable of recognizing specific targets and thus have been widely used for constructing various aptasensors.[162–177] Recently, nanozymes have been employed to develop numerous aptasensors for bioactive small molecules, proteins and metal ions.[154,157,159,160,178–183]

By making use of the AuNPs' peroxidase mimicking activities and an S-18 aptamer's high affinity and specificity to acetamiprid, a colorimetric assay for rapid pesticide monitoring was demonstrated.[159] The aptamer inhibited the nanozyme's activities due to its binding-induced surface passivation. Acetamiprid present in samples would interact with its aptamer and thus prevent the aptamer's binding onto AuNPs, which in turn recovered the AuNPs' catalytic activities. With Weerathunge's approach, as low as 0.1 ppm of acetamiprid was detected within 10 minutes, which met the requirement of the United States Environmental Protection Agency. The same group also showed their approach was applicable to a wide range of targets, such as antibiotics (kanamycin).[178]

Using the corresponding aptamers, several studies reported the detection of proteins, such as thrombin and lysozyme.[179–182] For example, sensitive and selective detection of thrombin was achieved in a recent study by Xu and coworkers.[180] The aptasensor for thrombin employed a multiple amplification strategy, in which peroxidase-like MnO_2 nanoflowers, PtNPs, toluidine blue, and hemin/G-quadruplex were co-assembled together onto multi-walled carbon nanotubes (CNTs). It was demonstrated that the designed multiple-catalysts were superior to other catalyst assemblies. The detection

of thrombin in 10-fold-diluted human blood serum was also demonstrated. Using DNA stabilized At/Pt nanoclusters as the peroxidase mimic, Zheng *et al.* reported a colorimetric aptasensor for thrombin detection.[181]

Based on the highly specific interaction between Hg^{2+} and T-rich DNA (*i.e.*, T–Hg^{2+}–T base pairing), Kim *et al.* reported a colorimetric approach for Hg^{2+} detection using the Fe_3O_4 MNP based peroxidase mimic.[160] The binding of T-rich DNA onto Fe_3O_4 MNPs inhibited the peroxidase mimicking activity. The presence of Hg^{2+} would recover the Fe_3O_4 MNPs' catalytic activity by Hg^{2+}-mediated release of T-rich DNA *via* T–Hg^{2+}–T coordination. In another study, it has been shown that G-rich DNA could enhance the AuNPs' peroxidase mimicking activity.[157] Since the G-rich DNA could specifically interact with K^+ by forming a G-quadruplex structure, a signal-off approach to K^+ detection was proposed.

In future, other functional nucleic acid-based sensing systems (such as DNAzyme-based sensors) should also be investigated, which will broaden the nanozyme research.[164,184]

2.6 Nanozymes for metal ion sensing

Quite a few studies have been devoted to metal ion sensing with nanozymes.[154,157,160,185–196] In an early report, a sensitive and selective sensor for Cu^{2+} was developed by using Cu^{2+}-based click chemistry.[185] *Via* the click chemistry, CNTs and magnetic silica nanoparticles were assembled together, leading to synergistic enhancement for CNTs' peroxidase mimicking activity. As low as 1 μM of Cu^{2+} was detected with the sensor.

As discussed above, Hg^{2+} has been detected based on T–Hg^{2+}–T coordination.[160] Other strategies were also studied for developing Hg^{2+} sensors.[186,190,193] For example, Li *et al.* prepared 2 nm PtNPs with BSA as the template and studied their peroxidase mimicking activity.[193] Interestingly, they found that Hg^{2+} specifically inhibited the nanozyme's activity due to Hg^{2+}–Pt^0 metallophilic interactions. They therefore developed a sensitive and selective sensor for Hg^{2+} detection. The sensor had a linear range of 0–120 nM and a detection limit of 7.2 nM. It has been applied for monitoring Hg^{2+} in drinking water. On the basis of the Ag^+ inhibition effect on $CoFe_2O_4$ nanoparticles' peroxidase mimicking activity, a chemiluminescent sensor for Ag^+ has been reported recently.[192]

2.7 Nanozymes for immunoassay

Enormous efforts have been made to develop immunoassays with nanozymes.[11,50,53,197–216]

Several formats have been employed for immunoassays using nanozymes as signalling elements. For example, Gao *et al.* reported an antigen-down immunoassay format and a capture-detection sandwich immunoassay format.[11] Later, many research groups adopted the classic sandwich immunoassay format for detection using peroxidase and oxidase mimicking nanozymes.[50,197,201,204,206,210,212] For example, Kim *et al.* prepared a highly active peroxidase mimic by encapsulating Fe_3O_4 MNPs and PtNPs within porous carbon.[206] They then used the nanozyme as the signalling element for labelling antibodies. With their nanozyme-labelled detection antibody, as low as 1.5 ng mL^{-1} of HER2 (human epidermal growth factor receptor 2) was detected within 3 minutes *via* a sandwich assay. Moreover, the diarrhea causing rotavirus was also successfully detected with the developed immunoassay. Gao and co-workers fabricated urchin-like Au@Pt core shell nanostructures as a highly efficient peroxidase mimic.[210] They then developed a sandwich assay for prostate specific antigen (PSA) detection. Using their nanozyme-labelled anti-PSA antibody as the detection antibody, as low as 2.9 pg mL^{-1} of PSA was determined. More excitingly, PSA concentrations in the clinical serum specimen were analyzed, which exhibited very good correlation with the referenced method. These studies suggested that nanozymes could be used as alternatives to conventional natural enzyme-based immunoassays in future.

Recently, several studies demonstrated that nanozymes can be used for point-of-care (POC) (Fig. 8).[207,211,213,216] To combat highly infectious diseases such as the Ebola virus, it is critical to perform rapid diagnosis, especially rapid local detection with portable devices. To meet this challenge, Duan and co-workers recently reported a nanozyme-based strip for Ebola virus detection, which exhibited 100 times more sensitivity compared to the AuNP-based strip (Fig. 8a).[211] They showed that as low as 240 pfu mL^{-1} of pseudo-EBOV could be detected within 30 minutes. As shown in Fig. 8b, Kim *et al.* developed a similar strip for hCG detection.[213] With the help of a smart phone (or other portable devices), the concentration of hCG could be readily quantified and communicated with patients/physicians and other clinical workers.

Catalase catalyzes the decomposition of H_2O_2 into H_2O and O_2 gas (Scheme 3). Though many nanomaterials have been used to mimic catalase, only a few studies have been focused on their applications.[1,207,216] Recently, Song *et al.* showed that the O_2 gas from catalase mimic-catalyzed H_2O_2 decomposition could be used for diagnosis (Fig. 8c).[207] They used PtNPs as the catalase mimic, which were then used to label the detection antibody for signalling. To efficiently and conveniently measure the produced O_2 gas, they developed a microfluidic platform called the volumetric bar-chart chip, which could easily gauge the volume of O_2 gas with coloured solution in the chip channel. With such a device, they have detected the cancer biomarker cytokeratin 19 fragment (CYFRA 21-1) in serum and HER2 expressed on three breast cancer cell surfaces. By pre-encapsulating the catalase mimic (*i.e.*, Au@PtNPs) within an aptamer hydrogel, Zhu and co-workers devised a similar bar-chart chip for cocaine detection (Fig. 8d).[216]

2.8 Nanozymes for detection of cells and bacteria

Cells (usually cancer cells) and bacteria have been detected with nanozymes.[53,198,202,205,209,217–220]

Cancer cells over-express characteristic receptors as cancer biomarkers. Therefore cancer cells can be detected with the corresponding antibodies or ligands, which recognize the receptors specifically. When an antibody or a ligand is

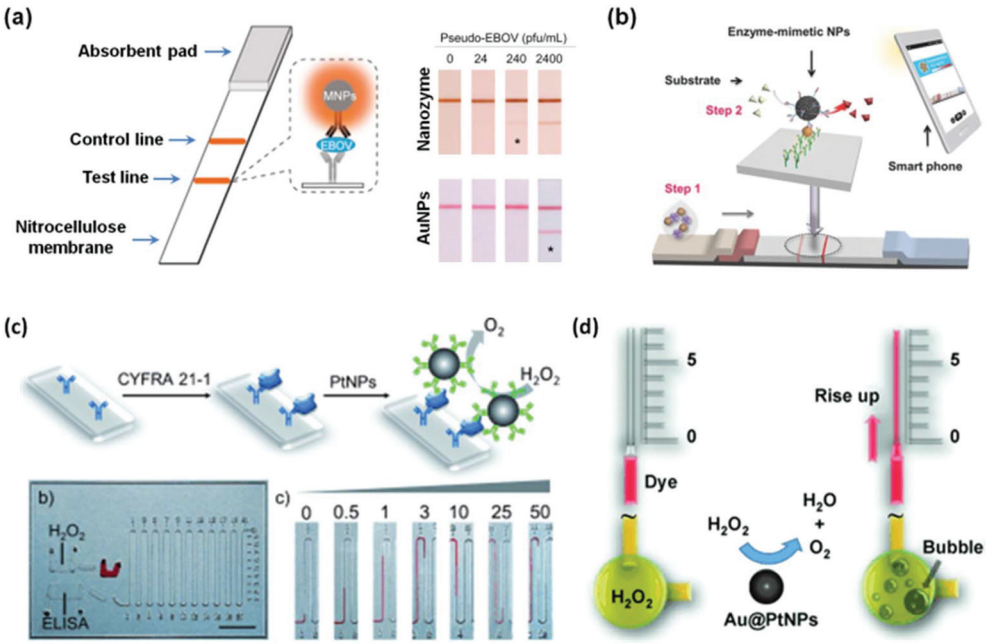

Fig. 8 Nanozymes for immunoassay. Nanozyme-based strips for Ebola detection using Fe_3O_4 MNPs as peroxidase mimic (a) and for hCG detection using hierarchically structured PtNPs as the peroxidase mimic (b). PtNPs (c) and Au@PtNPs (d) as catalase mimics for the immunoassay on a volumetric bar-chart chip. (a) Reprinted with permission from ref. 211. Copyright (2015) Elsevier. (b) Reprinted with permission from ref. 213. Copyright (2015) John Wiley and Sons. (c) Reprinted with permission from ref. 207. Copyright (2014) John Wiley and Sons. (d) Reprinted with permission from ref. 216. Copyright (2014) John Wiley and Sons.

$$2H_2O_2 \xrightarrow{\text{Catalase}} 2H_2O + O_2 \qquad (3)$$

Scheme 3 The reaction catalyzed by catalase.

conjugated with nanozymes, the conjugates can be employed for cancer cell detection. For example, Asati *et al.* employed antibody conjugated ceria nanoparticles for detection of folate receptor over-expressed lung carcinoma cells (A-549) and EpCAM over-expressed MCF-7 cells.[217] Recently, several studies also showed that folate receptor over-expressed cancer cells could be detected with various folate-modified nanozymes.[53,198,205,209] In Wang and co-workers' study, they discovered that chitosan stabilized silver halide (AgX) nanoparticles exhibited interesting peroxidase mimicking activities (Fig. 9a).[205] In the absence of H_2O_2, the AgX nanoparticles could still oxidize the substrate (such as TMB) if stimulated by light irradiation. Using AgI nanoparticles as the nanozyme, folate receptor over-expressed MDA-MB-231 cells were detected under light irradiation.

Wen reported the colorimetric detection of *Shewanella oneidensis*, a facultative anaerobic bacterium, on the basis of immunomagnetic capture of the bacteria and bacterial intrinsic peroxidase mimicking activities for signalling (Fig. 9b).[202] The developed method exhibited good selectivity toward *S. oneidensis* and has been used for identifying spiked *S. oneidensis* in river water.

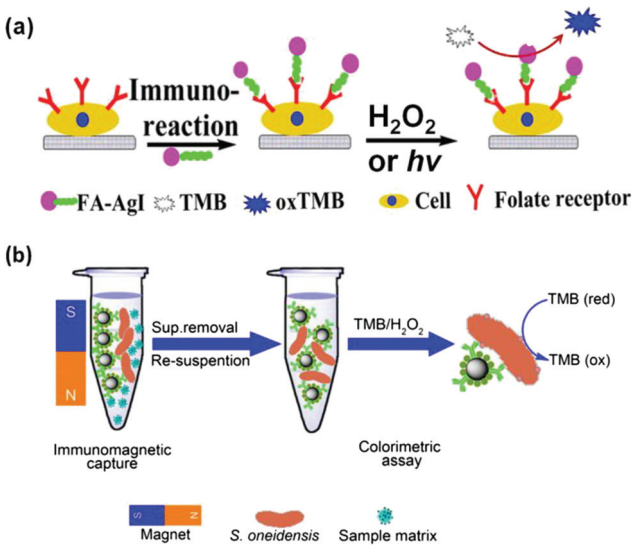

Fig. 9 Nanozymes for cancer cell (a) and bacterial detection (b). (a) Reprinted with permission from ref. 205. Copyright (2014) American Chemical Society. (b) Reprinted with permission from ref. 202. Copyright (2014) Nature Publishing Group.

2.9 Nanozymes for imaging

Fan *et al.* reported the imaging tumour tissue by staining them with magnetoferritin nanoparticles as a peroxidase mimic (Fig. 10).[221] Due to the presence of over-expressed transferrin

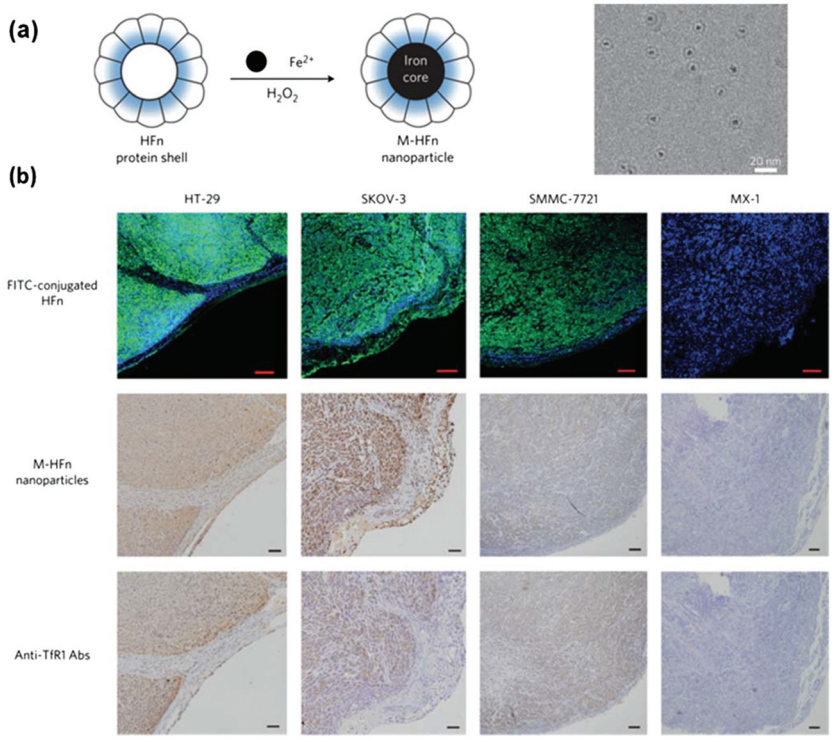

Fig. 10 Magnetoferritin nanoparticles as peroxidase mimic for tumour tissue staining and imaging. (a) Preparation of magnetoferritin nanoparticles. (b) Magnetoferritin nanoparticle staining of tumour tissues. Reprinted with permission from ref. 221. Copyright (2012) Nature Publishing Group.

receptor 1, the tumour tissues were specifically stained with the magnetoferritin nanoparticles, which were coated with recombinant human heavy-chain ferritin. For the 474 patient specimens examined, the nanozyme-based imaging technique successfully distinguished cancer samples from normal ones with a sensitivity of 98% and a specificity of 95%. Recently, Cai and co-workers also reported the staining and imaging tumour tissues with the magnetoferritin nanoparticles, which confirmed Fan's discovery.[208]

3. Nanozymes for therapeutics

By mainly eliminating reactive oxygen species (ROS) and/or reactive nitrogen species (RNS), nanozymes have been exploited for potential therapeutics.[13–17,25,209,222–237] The nanozymes' ROS scavenging capabilities mainly originated from their SOD mimicking activities, which convert superoxide into H_2O_2 (Scheme 4). In this section, the therapeutic effects of nanozymes are discussed, which cover anti-aging effects, anti-inflammatory effects, anti-oxidation effects, neuroprotection, promotion of stem cell growth, *etc*.

$$2O_2^{\bullet -} + 2H^+ \xrightarrow{\text{SOD}} H_2O_2 + O_2 \qquad (4)$$

Scheme 4 The reaction catalyzed by SOD.

3.1 Neuroprotection

Fullerene derivatives are among the first nanozymes used for therapeutic studies.[14,15] Dugan *et al.* pioneered the use of carboxyfullerenes as SOD mimics to protect neural cells from free radical damage.[14,15] In a later study, Dugan's group not only investigated the SOD mimicking activity of $C_{60}[C(COOH)_2]_3$ and the associated catalytic mechanism but also studied the nanozyme's therapeutic effect on SOD2 knockout mice (Fig. 11).[222] For the $Sod2^{-/-}$ mice, which cannot express mitochondrial manganese superoxide dismutase (MnSOD), their life span has been increased by 300% after either utero or postnatal treatment with the $C_{60}[C(COOH)_2]_3$ nanozyme. Since the nanozyme has been detected within mitochondria, it was proposed that the nanozyme may functionally replace MnSOD.

Ceria nanoparticles could also mimic SOD and exhibit interesting neuroprotective activity.[17,227,230] Chen and co-workers demonstrated that ceria nanoparticles could prevent retinal neuron cells from ROS damage, which was induced by intracellular hydrogen peroxide.[17] Remarkably, their animal studies also demonstrated that the ceria nanoparticle-based nanozyme exhibited protective activity towards light-induced rat retina photoreceptor cell degeneration.

ROS, generated and accumulated during ischemia, plays a critical role in ischemic stroke and associated neural injuries and diseases.[238] By eliminating the ischemic ROS, it would be possible to protect the brain against ischemic stroke. For the first time, Kim *et al.* demonstrated that PEGylated ceria nano-

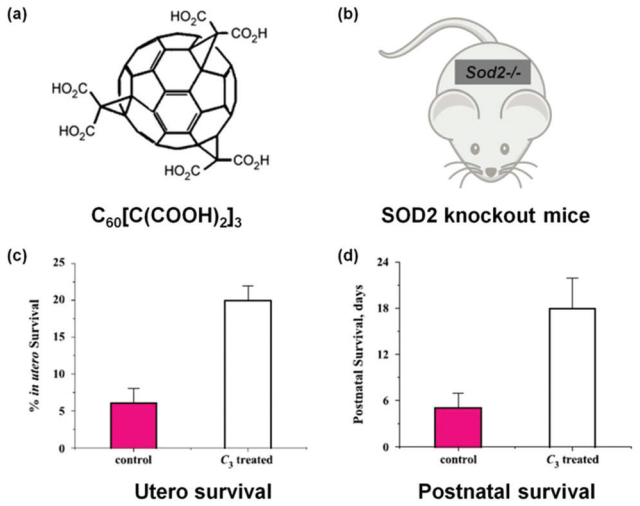

Fig. 11 Treatment of SOD2 knockout mice with $C_{60}[C(COOH)_2]_3$. (a) Structure of $C_{60}[C(COOH)_2]_3$. (b) SOD2 knockout mice. Utero (c) and postnatal (d) survival of SOD2 knockout mice after treatment with $C_{60}[C(COOH)_2]_3$. Adapted with permission from ref. 222. Copyright (2004) Elsevier.

particles indeed exhibited excellent protective activity against ischemic stroke.[227] The animal studies showed that ceria nanoparticles of optimal dosage reduced ischemic brain damage (Fig. 12).

RNS and amyloid beta (Aβ) peptides are involved in Alzheimer's disease (AD). However, effective therapy towards AD with suitable antioxidants is still lacking. To address this challenge, Dowding and co-workers studied the protective roles of nanoceria against RNS and Aβ-induced mitochondrial fragmentation and neuronal cell death.[230] The electron microscopic studies showed that the nanoceria were internalized by neurons and localized at the mitochondrial outer membrane and inner leaflet of the plasma membrane, where most of RNS were produced.[230] Due to the switchable oxidation states between Ce^{3+} and Ce^{4+}, ceria nanoparticles could scavenge RNS and thus protect the neurons against degeneration. The results demonstrated that ceria nanoparticles protected neurons from nitrosative-associated mitochondrial fragmentation, DRP1 S616 hyperphosphorylation and neuronal cell death.

Fig. 12 Ceria nanoparticles protect against ischemic stroke. Reprinted with permission from ref. 227. Copyright (2012) John Wiley and Sons.

3.2 Anti-aging

It is known that redox reactions participate in the aging process. For example, the detoxification of ROS is involved in regulating aging. Therefore, the ROS scavenging nanozymes may help to detoxify the ROS and thus prevent aging-related diseases. To this end, Quick *et al.* showed that the $C_{60}[C(COOH)_2]_3$-based SOD mimic exhibited interesting anti-aging effects and improved wild-type mice's cognition ability.[224] Detailed studies revealed that the nanozyme decreased the age-associated mitochondrial superoxide production and thus improved the mitochondrial biological function, which in turn rescued age-related cognitive impairment due to its localization within the mitochondria.[224]

3.3 Anti-inflammatory

ROS can induce inflammatory responses, which may lead to endothelial dysfunction and tissue injury.[239] By scavenging ROS with SOD or its mimics, it can protect cells and tissues from ROS-induced inflammation. Several nanozymes have exhibited interesting anti-inflammatory effects due to their ROS scavenging properties.[232,240] Hirst *et al.* studied the anti-inflammatory properties of ceria nanoparticles.[240] They demonstrated that the biocompatible ceria nanoparticles inhibited the production of ROS and radical nitric oxide (the two key inflammatory mediators) in J774A.1 murine macrophage cells. In a recent report, Son and co-workers integrated ceria nanoparticles as anti-inflammatory agents onto a bioresorbable electronic stent, which was a therapeutic device for endovascular diseases (Fig. 13).[232] Using human umbilical vein endothelial cells as a model, they demonstrated that the nanozyme was able to improve the cell viability under oxidative stress. Moreover, they showed that the nanozyme also exhibited excellent anti-inflammatory effects in animal models after implantation of the device in the canine common carotid artery. The nanozyme's anti-inflammatory properties were attributed to their ROS scavenging effect. This study offers a new direction for nanozyme research.

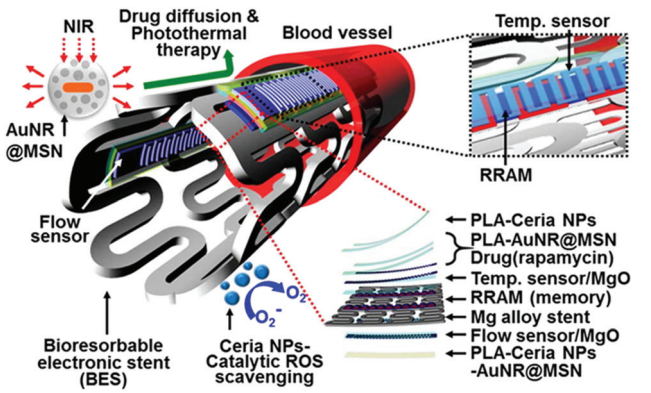

Fig. 13 Ceria nanoparticles as anti-inflammatory agents in a bioresorbable electronic stent for endovascular diseases. Reprinted with permission from ref. 232. Copyright (2015) American Chemical Society.

3.4 Anti-oxidation

The anti-oxidation effects of several nanozymes have been investigated.[13,234,241] Early studies demonstrated that the nanoceria possessed interesting anti-oxidation properties.[241] On the basis of the self-regenerating antioxidant mechanism, nanoceria protected cardiac progenitor cells from H_2O_2-induced cytotoxicity for one week.[241]

Su *et al.* examined the protective effects of PVP-stabilized iridium nanoparticles against H_2O_2-induced oxidative damage to A549 lung cancer cells.[234] They showed that IrNPs significantly reduced intracellular ROS levels and thus enhanced cell viability in a dose-dependent manner. Vernekar and coworkers studied the cytoprotective effect of vanadia (V_2O_5) nanowires (Fig. 14).[13] They found that the vanadia nanowires exhibited interesting glutathione peroxidase (GPx) mimicking activity (Fig. 14a). Moreover, by combining the nanozyme with glutathione reductase (GR), the GSH was recycled. Using the genetically encoded H_2O_2-specific probe HyPer, they showed that the nanozyme indeed exhibited ROS scavenging properties against both extrinsic H_2O_2 and intrinsic cellular peroxide (induced by $CuSO_4$) in HEK293T cells (Fig. 14b). The cytoprotective effects of the nanozyme were further confirmed by staining the cells with H_2O_2-specific dye Amplex Red and ROS-sensitive fluorescent dye DCFDA-H2 (Fig. 14c). In a following study, it was demonstrated that nanoceria could also mimic GPx and protect the cells *via* anti-oxidative effects.[233]

3.5 Anti-biofouling

Nanozymes have also been used for anti-biofouling.[231,242,243] Tremel's group discovered that vanadia nanowires could mimic haloperoxidase.[244] They further investigated the vanadia nanowires' anti-biofouling properties in a subsequent report.[242] They carried out a long-term (60 days) *in situ* study of the nanozyme's activity by fixing the testing samples to a boat hull. Remarkably, because of its excellent anti-biofouling activity, the nanozyme-coated stainless steel plates significantly prevented marine biofouling when compared with the uncoated stainless steel plate. Due to its high efficiency and low toxicity to marine biota, the nanozyme may be used as an alternative to conventional anti-biofouling agents.

Gao *et al.* recently studied the Fe_3O_4 MNP-enhanced oxidative cleavage of biofilm components (such as nucleic acids, proteins, oligosaccharides, and bacteria).[231] They used the Fe_3O_4 MNPs as a peroxidase mimic, which efficiently eliminated biofilms and thus prevented their formation in the presence of H_2O_2. Due to the nanozyme's unique penetrating properties into the protective, organic matrix, the developed Fe_3O_4 MNP–H_2O_2 system may provide a new approach to biofilm elimination in oral health, *etc.*

3.6 Other therapeutic applications

Nanozymes have also other interesting therapeutic potential, such as in promoting stem cell growth for tissue engineering and regulating iron homeostasis.[25,226,228,229,237,245–247]

In Kito's report, they investigated the effects of Fe_3O_4 MNPs-containing liposomes on the proliferation of induced pluripotent stem (iPS) cells (Fig. 15).[228] The proliferated iPS cells would form the cell sheets, which were then used for angiogenic cell therapy. It was found that the extracellular matrix (ECM) alone did not form a truly sheet-like structure and thus could not promote angiogenesis effectively. Surprisingly, when ECM was combined with Fe_3O_4 MNPs-containing liposomes for iPS cell proliferation, the formed iPS cell sheets significantly accelerated revascularization of the ischemic hindlimbs after implanting the sheets in nude mice. The Fe_3O_4 MNP-enhanced angiogenesis was attributed to the peroxidase-like anti-oxidative activities. The presence of Fe_3O_4 MNPs also improved the sheets' mechanical properties, provid-

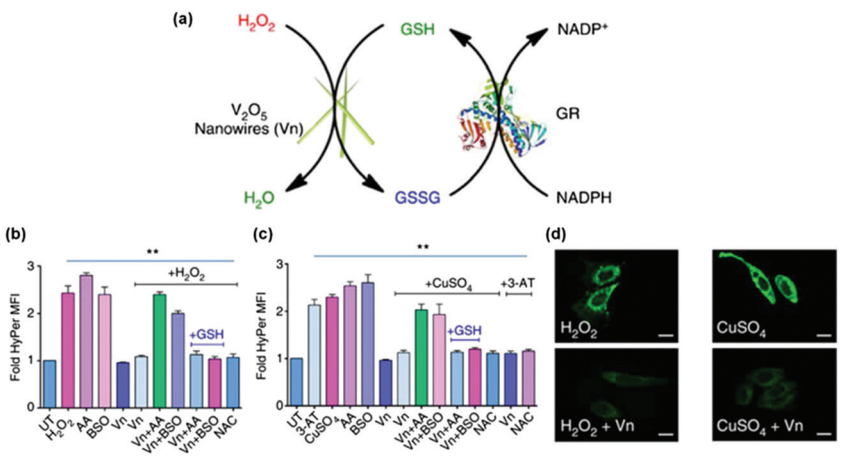

Fig. 14 Vanadia nanowires as anti-oxidation nanozymes for cytoprotection. (a) Schematic depicting the glutathione peroxidase (GPx)-like antioxidant activity of vanadia nanowires (Vn) and GSH recycling by glutathione reductase (GR). Extrinsic H_2O_2 (b) and intrinsic cellular peroxide (induced by $CuSO_4$) (c) scavenging activities of Vn measured using genetically encoded H_2O_2-specific probe HyPer in HEK293T cells. Cells were either left untreated or pretreated with various agents. (d) HeLa cells were treated with Vn before the treatment with H_2O_2 or $CuSO_4$ and then stained with 15 μM DCFDA-H2 dye. Reprinted with permission from ref. 13. Copyright (2014) Nature Publishing Group.

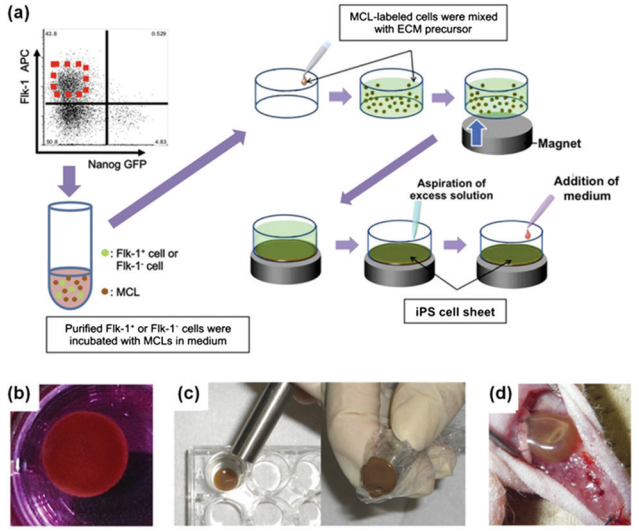

Fig. 15 Fe_3O_4 MNP-facilitated formation of iPS cell sheets for reparative angiogenesis. (a) Procedure for construction of iPS cell-derived cell sheet. (b) An alnico magnet was positioned on the surface of the culture medium. The Flk-1 cell sheet floated up to the surface of the culture medium without disruption. (c) The magnetized Flk-1 cell sheet attached to an Alnico magnet covered with polyvinylidene difluoride membrane *via* a magnetic force. (d) Flk-1 cell sheets were placed on the adductor muscles of nude mice using the Alnico magnet. Reprinted with permission from ref. 228. Copyright (2013) Nature Publishing Group.

ing sufficient strength for handling.[228] This study provides an interesting approach to tissue engineering for reparative angiogenesis.

Li *et al.* prepared PtNPs within L-chain apoferritin cages, which showed ferroxidase mimicking activity.[25] They further showed that the nanozyme could regulate iron homeostasis, providing great promise for therapeutic applications. Molybdenum trioxide nanoparticles exhibited sulfite oxidase mimicking activity.[229] The cellular study showed that the nanozyme could act as an alternative to natural sulfite oxidase, suggesting the potential use for treating sulfite oxidase-defect diseases.

4. Other applications

Nanozymes have also found other exciting applications, such as in constructing logic gates, pollutant removal and water treatment, *etc.*[23,65,187,189,247–255]

4.1 Logic gates

Several logic gates have been constructed with various nanozymes.[187,189,248,249]

As shown in Fig. 16, when the ceria nanoparticles were combined with natural enzymes, label-free, resettable, and colorimetric logic gates have been fabricated.[248] For ceria nanoparticles, they were colourless when Ce^{3+} was dominant on the nanoparticles' surface. However, they would turn into yellow

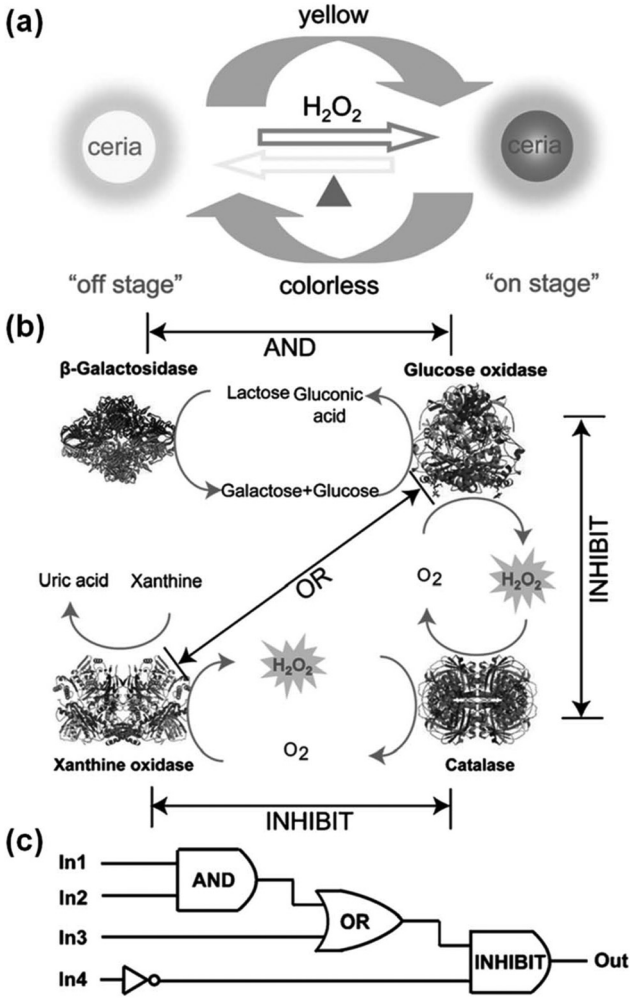

Fig. 16 Ceria nanoparticles for colorimetric logic gates. (a) Illustration of a thermally responsive switch based on CeO_2 nanoparticles. (b) The operation of logic gates based on biocatalytic reactions. (c) Logic circuitry for the integrated logic system. In1 = β-galactosidase, In2 = glucose oxidase, In3 = xanthine oxidase, In4 = catalase. Reprinted with permission from ref. 248. Copyright (2012) John Wiley and Sons.

colour when the surface Ce^{3+} was oxidized to Ce^{4+} with H_2O_2. Moreover, by heating, the yellow coloured ceria nanoparticles would return to colourless (Fig. 16a). Lin *et al.* exploited the unique colour change of the ceria nanoparticles as a signalling readout to construct various logic gates. For example, when the ceria nanoparticles were combined with β-galactosidase and glucose oxidase, an "AND" logic gate was built, and "OR" and "INHIBIT" logic gates were also obtained (Fig. 16c). Due to the thermally responsive colour changing properties, the ceria nanoparticles could be transformed into colourless ones, which in turn reset the logic gates. The potential application of the logic gates for multiplex detection was also studied.

Lien and co-workers reported several logic gates on the basis of tuning the AuNPs' multiple enzyme-like activities with metal ions.[187,189] For example, both Be^{3+} and Hg^{2+} enhanced AuNPs' catalase mimicking activity, respectively. Thus, an

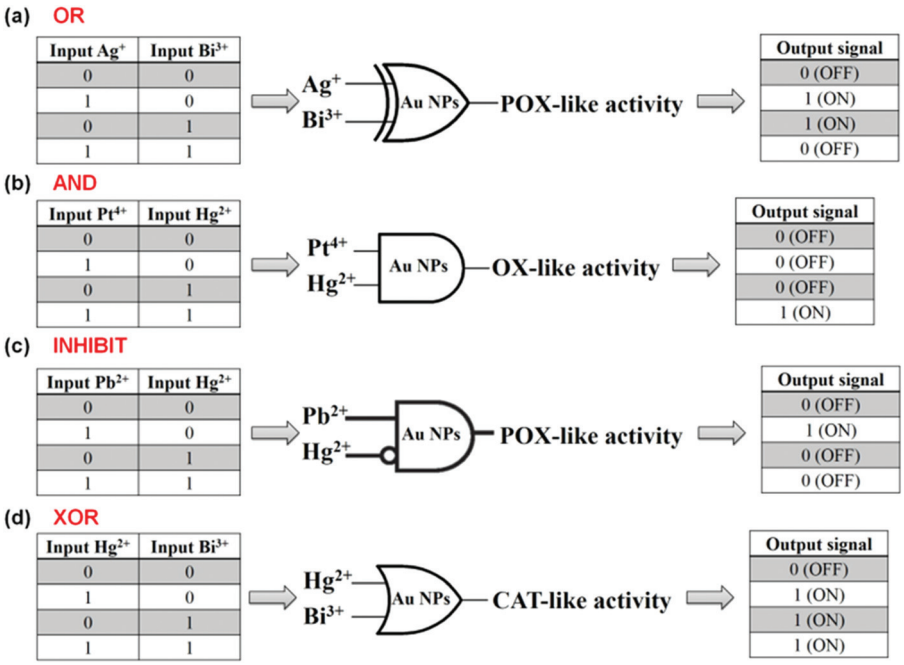

Fig. 17 Logical regulation of the enzyme-like activity of AuNPs by using metal ions. "OR" (a), "AND" (b), "INHIBIT" (c), and "XOR" (d) logic gates on the basis of tuning AuNPs' enzyme mimicking activities with various metal ions. Reprinted with permission from ref. 187. Copyright (2013) Royal Society of Chemistry.

"OR" logic gate was developed using Be^{3+} and Hg^{2+} as inputs and the AuNPs' catalase activity as the output (Fig. 17a).[187] To enhance the AuNPs' oxidase mimicking activity, both Pt^{4+} and Hg^{2+} were necessary. On the basis of this phenomenon, an "AND" logic gate was fabricated (Fig. 17b). Similarly, an "INHIBIT" logic gate was developed by tuning AuNPs' peroxidase mimicking activity with Pb^{2+} and Hg^{2+} (Fig. 17c). Pb^{2+} enhanced the peroxidase mimicking activity while Hg^{2+} exhibited an inhibition effect. The presence of both Pb^{2+} and Hg^{2+}, however, also inhibited the mimicking activity. An "XOR" logic gate was also reported by tuning the AuNPs' peroxidase mimicking activity with Hg^{2+} and Bi^{3+} (Fig. 17d).

4.2 Pollutant removal and water treatment

Yan's group reported the removal of phenolic pollutants from aqueous solutions using the Fe_3O_4 MNP-based peroxidase mimic.[250] After that, numerous studies have been devoted to pollutant removal and water treatment with nanozymes.[23,65,250–252]

In a recent report, Janos *et al.* investigated the phosphatase mimicking behaviour of the CeO_2/γ-Fe_2O_3 nanocomposites.[23] Due to the adsorption and phosphatase mimetic properties, the nanozyme has been used to decompose organophosphorus pesticide parathion methyl as well as the chemical warfare agents Soman and VX at ambient temperature. Since the nanozyme still retained the magnetic properties, it could be recycled and used in various decontamination strategies.[23]

5. Mechanisms

Though relatively few studies have been focused on elucidating the mechanisms of the nanozyme based catalysis, several mechanisms have been established.[32,222] In this section, the catalytic mechanisms of the fullerene-based SOD mimic and the nanoceria-based SOD and catalase mimics are discussed, which should be helpful for understanding the mechanisms of other nanozymes in the future.

5.1 $C_{60}[C(COOH)_2]_3$ based SOD mimic

The detailed mechanism of $C_{60}[C(COOH)_2]_3$ based SOD mimic has been proposed by Ali and co-workers.[222] By combining the experimental results (such as electron paramagnetic resonance (EPR) measurements and kinetics studies) with semiempirical quantum-mechanical calculations, they proposed the mechanism shown in Fig. 18.[222] Their study suggested that the electron-deficient regions on the $C_{60}[C(COOH)_2]_3$ nanozyme attracted the substrate anions (*i.e.*, $O_2^{\bullet-}$) towards the surface of the nanozyme electrostatically and then directed the substrate for further dismutation. The whole process was facilitated by the protons from the carboxyl groups of the nanozyme and/or surrounding water molecules around the nanozyme.[222]

5.2 Nanoceria based SOD mimic

The SOD mimetic activity of nanoceria has been validated by the competitive assay against cytochrome c.[256] Based on EPR measurements, kinetics studies as well as other observations, Self's group proposed a dismutation mechanism of nanoceria-

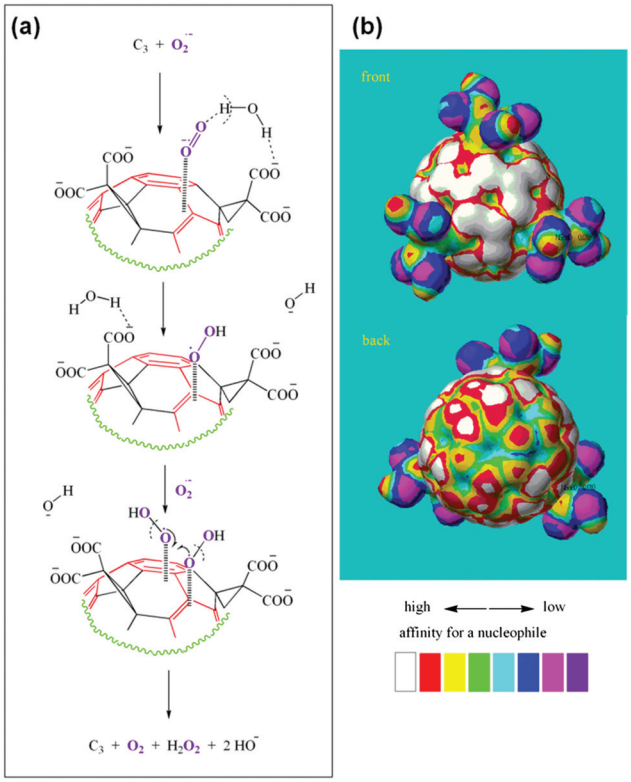

Fig. 18 Proposed mechanism of $C_{60}[C(COOH)_2]_3$ based SOD mimic. Reprinted with permission from ref. 222. Copyright (2004) Elsevier.

based SOD mimics, which is similar to the mechanism of Fe- and Mn-SOD.[256] As shown in Fig. 19, an alternative mechanism was proposed by Celardo *et al.*, which showed the redox cycle between Ce^{3+} and Ce^{4+}.[32]

5.3 Nanoceria based catalase mimic

Nanoceria has also shown catalase mimetic activity. Fig. 20 shows a possible mechanism for the reaction cycle similar to

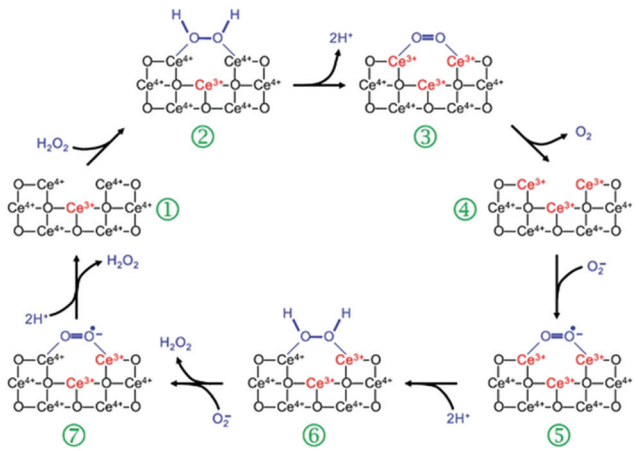

Fig. 19 Proposed mechanism of nanoceria based SOD mimic. Reprinted with permission from ref. 32. Copyright (2011) Royal Society of Chemistry.

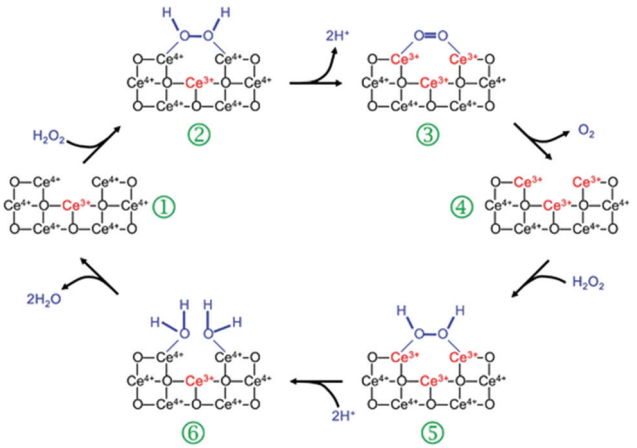

Fig. 20 Proposed mechanism of nanoceria based catalase mimic. Reprinted with permission from ref. 32. Copyright (2011) Royal Society of Chemistry.

the one of natural catalase.[32] The overall reaction involved in Fig. 20 can be expressed by eqn (3) in Scheme 3.

6. Summary and outlook

This review highlights the recent progress of nanozymes, especially their applications in bionanotechnology. Using selected examples, the broad applications in various areas (such as sensing, imaging, therapeutics, logic gates, pollutant removal and water treatment) were discussed.

As evidenced by the above-mentioned examples, the research field of nanozymes has grown substantially. To fulfill their great potential however, there are still numerous challenges remaining to be tackled.[1]

First, though many nanomaterials have been exploited to mimic various natural enzymes,[81,101,257–267] currently the redox enzyme mimics are still dominant in the developed nanozymes. Therefore, new strategies are needed to design and prepare other types of nanozymes. Recent progress in theoretical and computational protein design has enabled the design of new functional proteins, including enzymes.[268,269] Such an approach should also be applicable to nanozyme design by combining experiments with theoretical and/or computational strategies.

Second, nanozymes are superior to natural enzymes in their enhanced stability, recyclability, low-cost, *etc.*[105,270] Their catalytic activity and selectivity, however, still cannot compete with natural enzymes. By further understanding their mechanisms, high-performance nanozymes could be rationally designed in future.[271–274] For example, by taking advantage of the synergistic effect, nanozymes with improved activities have been prepared.[275]

Third, natural enzymes usually work together within a confined environment. To truly mimic natural enzymes, cascade reactions catalyzed by nanozyme assemblies (or assemblies of

nanozyme and natural enzyme) should be further exploited.[238,276,277]

Fourth, like natural enzymes, nanozyme' activities can be regulated.[47,78,158,278–285] For example, by tailoring the nanozymes' composition, their activities could be tuned.[78,278] pH and even light have been investigated for modulating the nanozymes' activities.[280,281,283,284] Despite the current progress, more approaches and factors are still needed to intentionally modulate nanozymes' catalytic properties. Among them, biomolecules will play critical roles in manipulating nanozymes' catalytic behaviours.[47,158,286–290]

Fifth, for biomedical applications, a broader range of targets should be considered. More importantly, translational studies should be carried out whenever possible in future. For example, when the nanozyme-based test strips are combined with available telemed devices, they may help us address the need for point-of-care and even precision medicine. For the therapeutic nanozymes, their effective windows should be carefully optimized to avoid potential toxicity.

Sixth, for biomedical applications, the toxicity of nanozymes should be systematically studied. Though previous reports have shown that several nanozymes have been employed for therapeutic studies in animal models, their translation into clinical applications remains a great challenge. Currently, a few FDA approved superparamagnetic iron oxide nanoparticles, such as Resovist (Ferucarbotran), have exhibited peroxidase-like activity and been used for promoting stem cell proliferation.[237] However, the toxicity of other promising nanozymes should be tested for clinical trials.

Finally, chiral catalysis using nanozyme has been reported recently.[255] Here we speculate that nanozymes may be even involved in the origin of life since there must have been some catalysts to carry out the catalysis before biocatalysts evolved.

Abbreviations

4-AAP	4-Minoantipyrine
ABTS	2,2′-Azino-bis(3-ethylbenzothiazoline-6-sulphonic acid)
CNTs	Carbon nanotubes
DPD	*N*,*N*-Diethyl-*p*-phenylenediamine
DRP1	Dynamin-related protein 1
ECM	Extracellular matrix
EpCAM	Epithelial cell adhesion molecule
EPR	Electron paramagnetic resonance
FDA	Food and drug administration
GPx	Glutathione peroxidase
GSH	Glutathione
hCG	Human chorionic gonadotropin
HER2	Human epidermal growth factor receptor 2
5-HIAA	5-Hydroxyindole-3-acetic acid
HPLC	High-performance liquid chromatography
iPS	Induced pluripotent stem
LOD	Limit of detection
MNPs	Magnetic nanoparticles
MS	Mass spectrometry
NPs	Nanoparticles
OPD	*o*-Phenylenediamine
POC	Point-of-care
PSA	Prostate specific antigen
PVP	Polyvinylpyrrolidone
rGO	Reduced graphene oxide
SERS	Surface enhanced Raman scattering
SOD	Superoxide dismutase
TMB	3,3′,5,5′-Tetramethylbenzidine

Acknowledgements

We thank the National Natural Science Foundation of China (no. 21405081), the Natural Science Foundation of Jiangsu Province (no. BK20130561), the 973 Program (no. 2015CB659400), the 985 Program of Nanjing University, the Priority Academic Program Development of Jiangsu Higher Education Institutions (PAPD), the Shuangchuang Program of Jiangsu Province, the Six Talents Summit Program of Jiangsu Province, Fundamental Research Funds for the Central Universities, Open Funds of the State Key Laboratory of Electroanalytical Chemistry (SKLEAC201501), and the Thousand Talents Program for Young Researchers for financial support.

Notes and references

1 H. Wei and E. K. Wang, *Chem. Soc. Rev.*, 2013, **42**, 6060–6093.
2 L. Z. Gao and X. Y. Yan, *Prog. Biochem. Biophys.*, 2013, **40**, 892–902.
3 L. Pasquato, P. Pengo and P. Scrimin, *Supramol. Chem.*, 2005, **17**, 163–171.
4 L. Z. Gao and X. Y. Yan, in *Nanomaterials: emerging characteristics and biomedical applications*, ed. X. Y. Yan, Science Press, Beijing, 2014.
5 T. Pirmohamed, J. M. Dowding, S. Singh, B. Wasserman, E. Heckert, A. S. Karakoti, J. E. S. King, S. Seal and W. T. Self, *Chem. Commun.*, 2010, **46**, 2736–2738.
6 S. Singh, T. Dosani, A. S. Karakoti, A. Kumar, S. Seal and W. T. Self, *Biomaterials*, 2011, **32**, 6745–6753.
7 W. W. He, Y. Liu, J. S. Yuan, J. J. Yin, X. C. Wu, X. N. Hu, K. Zhang, J. B. Liu, C. Y. Chen, Y. L. Ji and Y. T. Guo, *Biomaterials*, 2011, **32**, 1139–1147.
8 Z. W. Chen, J. J. Yin, Y. T. Zhou, Y. Zhang, L. Song, M. J. Song, S. L. Hu and N. Gu, *ACS Nano*, 2012, **6**, 4001–4012.
9 M. Comotti, C. Della Pina, R. Matarrese and M. Rossi, *Angew. Chem., Int. Ed.*, 2004, **43**, 5812–5815.
10 A. Asati, S. Santra, C. Kaittanis, S. Nath and J. M. Perez, *Angew. Chem., Int. Ed.*, 2009, **48**, 2308–2312.
11 L. Z. Gao, J. Zhuang, L. Nie, J. B. Zhang, Y. Zhang, N. Gu, T. H. Wang, J. Feng, D. L. Yang, S. Perrett and X. Yan, *Nat. Nanotechnol.*, 2007, **2**, 577–583.

12 H. Wei and E. Wang, *Anal. Chem.*, 2008, **80**, 2250–2254.
13 A. A. Vernekar, D. Sinha, S. Srivastava, P. U. Paramasivam, P. D'Silva and G. Mugesh, *Nat. Commun.*, 2014, **5**, 5301.
14 L. L. Dugan, J. K. Gabrielsen, S. P. Yu, T. S. Lin and D. W. Choi, *Neurobiol. Dis.*, 1996, **3**, 129–135.
15 L. L. Dugan, D. M. Turetsky, C. Du, D. Lobner, M. Wheeler, C. R. Almli, C. K. F. Shen, T. Y. Luh, D. W. Choi and T. S. Lin, *Proc. Natl. Acad. Sci. U. S. A.*, 1997, **94**, 9434–9439.
16 R. W. Tarnuzzer, J. Colon, S. Patil and S. Seal, *Nano Lett.*, 2005, **5**, 2573–2577.
17 J. P. Chen, S. Patil, S. Seal and J. F. McGinnis, *Nat. Nanotechnol.*, 2006, **1**, 142–150.
18 H. Tokuyama, S. Yamago, E. Nakamura, T. Shiraki and Y. Sugiura, *J. Am. Chem. Soc.*, 1993, **115**, 7918–7919.
19 A. S. Boutorine, H. Tokuyama, M. Takasugi, H. Isobe, E. Nakamura and C. Helene, *Angew. Chem., Int. Ed. Engl.*, 1995, **33**, 2462–2465.
20 S. Bosi, T. Da Ros, G. Spalluto and M. Prato, *Eur. J. Med. Chem.*, 2003, **38**, 913–923.
21 L. Pasquato, F. Rancan, P. Scrimin, F. Mancin and C. Frigeri, *Chem. Commun.*, 2000, 2253–2254.
22 F. Manea, F. B. Houillon, L. Pasquato and P. Scrimin, *Angew. Chem., Int. Ed.*, 2004, **43**, 6165–6169.
23 P. Janos, P. Kuran, V. Pilarova, J. Trogl, M. Stastny, O. Pelant, J. Henych, S. Bakardjieva, O. Zivotsky, M. Kormunda, K. Mazanec and M. Skoumal, *Chem. Eng. J.*, 2015, **262**, 747–755.
24 B. Li, D. M. Chen, J. Q. Wang, Z. Y. Yan, L. Jiang, D. L. Duan, J. He, Z. R. Luo, J. P. Zhang and F. G. Yuan, *Sci. Rep.*, 2014, **4**, 6759.
25 L. Li, L. Zhang, U. Carmona and M. Knez, *Chem. Commun.*, 2014, **50**, 8021–8023.
26 X. Li, F. Wen, B. Creran, Y. Jeong, X. Zhang and V. M. Rotello, *Small*, 2012, **8**, 3589–3592.
27 E. Nakamura and H. Isobe, *Acc. Chem. Res.*, 2003, **36**, 807–815.
28 W. He, W. Wamer, Q. Xia, J.-j. Yin and P. P. Fu, *J. Environ. Sci. Health Environ. Part C: Environ Carcinog. Ecotoxicol. Rev.*, 2014, **32**, 186–211.
29 L. J. Prins, *Acc. Chem. Res.*, 2015, **48**, 1920–1928.
30 Y. H. Lin, J. S. Ren and X. G. Qu, *Adv. Mater.*, 2014, **26**, 4200–4217.
31 J. X. Xie, X. D. Zhang, H. Wang, H. Z. Zheng and Y. M. Huang, *TrAC, Trends Anal. Chem.*, 2012, **39**, 114–129.
32 I. Celardo, J. Z. Pedersen, E. Traversa and L. Ghibelli, *Nanoscale*, 2011, **3**, 1411–1420.
33 L. Zheng, J. Zhao, X. Niu and Y. Yang, *Mater. Rev.*, 2015, **29**, 115.
34 Y. H. Lin, J. S. Ren and X. G. Qu, *Acc. Chem. Res.*, 2014, **47**, 1097–1105.
35 A. Karakoti, S. Singh, J. M. Dowding, S. Seal and W. T. Self, *Chem. Soc. Rev.*, 2010, **39**, 4422–4432.
36 C. Xu and X. G. Qu, *NPG Asia Mater.*, 2014, **6**, e90.
37 C. L. Guo, Y. H. Song, H. Wei, P. C. Li, L. Wang, L. L. Sun, Y. J. Sun and Z. Li, *Anal. Bioanal. Chem.*, 2007, **389**, 527–532.
38 Z. Liu, B. Zhao, Y. Shi, C. Guo, H. Yang and Z. Li, *Talanta*, 2010, **81**, 1650–1654.
39 K. Zhao, W. Gu, S. S. Zheng, C. L. Zhang and Y. Z. Xian, *Talanta*, 2015, **141**, 47–52.
40 Y. H. Wang, B. Zhou, S. Wu, K. M. Wang and X. X. He, *Talanta*, 2015, **134**, 712–717.
41 F. M. Qiao, L. J. Chen, X. N. Li, L. F. Li and S. Y. Ai, *Sens. Actuators, B*, 2014, **193**, 255–262.
42 A. K. Dutta, S. K. Maji, A. Mondal, B. Karmakar, P. Biswas and B. Adhikary, *Sens. Actuators, B*, 2012, **173**, 724–731.
43 Y. F. Zhang, C. L. Xu and B. X. Li, *RSC Adv.*, 2013, **3**, 6044–6050.
44 W. S. Yang, J. H. Hao, Z. Zhang, B. P. Lu, B. L. Zhang and J. L. Tang, *RSC Adv.*, 2014, **4**, 35500–35504.
45 P. C. Pandey, D. Panday and G. Pandey, *RSC Adv.*, 2014, **4**, 60563–60572.
46 A. Dalui, B. Pradhan, U. Thupakula, A. H. Khan, G. S. Kumar, T. Ghosh, B. Satpati and S. Acharya, *Nanoscale*, 2015, **7**, 9062–9074.
47 L. J. Chen, K. F. Sun, P. P. Li, X. Z. Fan, J. C. Sun and S. Y. Ai, *Nanoscale*, 2013, **5**, 10982–10988.
48 Q. Chang and H. Q. Tang, *Microchim. Acta*, 2014, **181**, 527–534.
49 Q. Y. Liu, L. Y. Zhang, H. Li, Q. Y. Jia, Y. L. Jiang, Y. T. Yang and R. R. Zhu, *Mater. Sci. Eng., C*, 2015, **55**, 193–200.
50 W. Zhang, Y. Zhang, Y. H. Chen, S. Y. Li, N. Gu, S. L. Hu, Y. Sun, X. Chen and Q. Li, *J. Nanosci. Nanotechnol.*, 2013, **13**, 60–67.
51 D. Wu, X. Deng, X. M. Huang, K. Wang and Q. Y. Liu, *J. Nanosci. Nanotechnol.*, 2013, **13**, 6611–6616.
52 R. Z. Zhang, S. J. He, C. M. Zhang and W. Chen, *J. Mater. Chem. B*, 2015, **3**, 4146–4154.
53 C. L. Sun, X. L. Chen, J. Xu, M. J. Wei, J. J. Wang, X. G. Mi, X. H. Wang, Y. Wu and Y. Liu, *J. Mater. Chem. A*, 2013, **1**, 4699–4705.
54 T. H. Han, M. M. Khan, J. Lee and M. H. Cho, *J. Ind. Eng. Chem.*, 2014, **20**, 2003–2009.
55 L. Zhan, Y. Zhang, Q. L. Zeng, Z. D. Liu and C. Z. Huang, *J. Colloid Interface Sci.*, 2014, **426**, 293–299.
56 X. Yang, L. N. Wang, G. Z. Zhou, N. Sui, Y. X. Gu and J. Wan, *J. Cluster Sci.*, 2015, **26**, 789–798.
57 Y. Gao, Z. Wei, F. Li, Z. M. Yang, Y. M. Chen, M. Zrinyi and Y. Osada, *Green Chem.*, 2014, **16**, 1255–1261.
58 S. H. Ma, X. J. Wang and X. J. Han, *Chin. J. Anal. Chem.*, 2013, **41**, 1719–1723.
59 W. T. Yao, H. Z. Zhu, W. G. Li, H. B. Yao, Y. C. Wu and S. H. Yu, *ChemPlusChem*, 2013, **78**, 723–727.
60 T. Wang, Y. C. Fu, L. Y. Chai, L. Chao, L. J. Bu, Y. Meng, C. Chen, M. Ma, Q. J. Xie and S. Z. Yao, *Chem. – Eur. J.*, 2014, **20**, 2623–2630.
61 F. X. Qin, S. Y. Jia, F. F. Wang, S. H. Wu, J. Song and Y. Liu, *Catal. Sci. Technol.*, 2013, **3**, 2761–2768.

62 A. X. Zheng, Z. X. Cong, J. R. Wang, J. Li, H. H. Yang and G. N. Chen, *Biosens. Bioelectron.*, 2013, **49**, 519–524.
63 Q. Y. Liu, Y. T. Yang, H. Li, R. R. Zhu, Q. Shao, S. G. Yang and J. J. Xu, *Biosens. Bioelectron.*, 2015, **64**, 147–153.
64 A. L. Hu, Y. H. Liu, H. H. Deng, G. L. Hong, A. L. Liu, X. H. Lin, X. H. Xia and W. Chen, *Biosens. Bioelectron.*, 2014, **61**, 374–378.
65 Y. Pan, N. Li, J. S. Mu, R. H. Zhou, Y. Xu, D. Z. Cui, Y. Wang and M. Zhao, *Appl. Microbiol. Biotechnol.*, 2015, **99**, 703–715.
66 J. F. Guan, J. Peng and X. Y. Jin, *Anal. Methods*, 2015, **7**, 5454–5461.
67 H. T. Fang, Y. L. Pan, W. Q. Shan, M. L. Guo, Z. Nie, Y. Huang and S. Z. Yao, *Anal. Methods*, 2014, **6**, 6073–6081.
68 A. D. Ryabov, R. Ceron-Camacho, O. Saavedra-Diaz, M. A. Denardo, A. Ghosh, R. Le Lagadec and T. J. Collins, *Anal. Chem.*, 2012, **84**, 9096–9100.
69 L. P. Lin, X. H. Song, Y. Y. Chen, M. C. Rong, T. T. Zhao, Y. R. Wang, Y. Q. Jiang and X. Chen, *Anal. Chim. Acta*, 2015, **869**, 89–95.
70 F. M. Qiao, Z. Z. Wang, K. Xu and S. Y. Ai, *Analyst*, 2015, **140**, 6684–6691.
71 Q. Chen, J. Chen, C. J. Gao, M. L. Zhang, J. Y. Chen and H. D. Qiu, *Analyst*, 2015, **140**, 2857–2863.
72 Y. Shi, P. Su, Y. Y. Wang and Y. Yang, *Talanta*, 2014, **130**, 259–264.
73 F. T. Zhang, X. Long, D. W. Zhang, Y. L. Sun, Y. L. Zhou, Y. R. Ma, L. M. Qi and X. X. Zhang, *Sens. Actuators, B*, 2014, **192**, 150–156.
74 F. M. Qian, J. M. Wang, S. Y. Ai and L. F. Li, *Sens. Actuators*, 2015, **216**, 418–427.
75 F. Pogacean, C. Socaci, S. Pruneanu, A. R. Biris, M. Coros, L. Magerusan, G. Katona, R. Turcu and G. Borodi, *Sens. Actuators, B*, 2015, **213**, 474–483.
76 X. M. Chen, B. Y. Su, Z. X. Cai, X. Chen and M. Oyama, *Sens. Actuators, B*, 2014, **201**, 286–292.
77 P. C. Pandey, R. Singh and Y. Pandey, *RSC Adv.*, 2015, **5**, 49671–49679.
78 J. Q. Tian, Q. Liu, A. M. Asiri, A. H. Qusti, A. O. Al-Youbi and X. P. Sun, *Nanoscale*, 2013, **5**, 11604–11609.
79 P. Gayathri and A. S. Kumar, *Chem. – Eur. J.*, 2013, **19**, 17103–17112.
80 L. H. Ai, L. L. Li, C. H. Zhang, J. Fu and J. Jiang, *Chem. – Eur. J.*, 2013, **19**, 15105–15108.
81 Y. Tao, E. G. Ju, J. S. Ren and X. G. Qu, *Chem. Commun.*, 2014, **50**, 3030–3032.
82 K. S. McKeating, S. Sloan-Dennison, D. Graham and K. Faulds, *Analyst*, 2013, **138**, 6347–6353.
83 T. B. Zhang, Y. C. Lu and G. S. Luo, *ACS Appl. Mater. Interfaces*, 2014, **6**, 14433–14438.
84 J. A. R. Guivar, E. G. R. Fernandes and V. Zucolotto, *Talanta*, 2015, **141**, 307–314.
85 J. Zhuang, J. B. Zhang, L. Z. Gao, Y. Zhang, N. Gu, J. Feng, D. L. Yang and X. Y. Yan, *Mater. Lett.*, 2008, **62**, 3972–3974.
86 S. Chen, X. Hai, X. W. Chen and J. H. Wang, *Anal. Chem.*, 2014, **86**, 6689–6694.
87 D. Antuna-Jimenez, M. C. Blanco-Lopez, A. J. Miranda-Ordieres and M. J. Lobo-Castanon, *Polymer*, 2014, **55**, 1113–1119.
88 Y. Shi, J. Huang, J. N. Wang, P. Su and Y. Yang, *Talanta*, 2015, **143**, 457–463.
89 A. K. Dutta, S. Das, S. Samanta, P. K. Samanta, B. Adhikary and P. Biswas, *Talanta*, 2013, **107**, 361–367.
90 Q. Li, G. G. Tang, X. W. Xiong, Y. L. Cao, L. L. Chen, F. G. Xu and H. L. Tan, *Sens. Actuators, B*, 2015, **215**, 86–92.
91 A. K. Dutta, S. K. Maji, P. Biswas and B. Adhikary, *Sens. Actuators, B*, 2013, **177**, 676–683.
92 W. F. Dong, X. D. Liu, W. B. Shi and Y. M. Huang, *RSC Adv.*, 2015, **5**, 17451–17457.
93 J. Huang, Q. Chang, G. Jiang, Y. Qiu and H. Tang, *Phys. Test. Chem. Anal. B Chem. Anal.*, 2014, **50**, 417–420.
94 T. R. Lin, L. S. Zhong, L. Q. Guo, F. F. Fu and G. N. Chen, *Nanoscale*, 2014, **6**, 11856–11862.
95 L. Han, L. X. Zeng, M. D. Wei, C. M. Li and A. H. Liu, *Nanoscale*, 2015, **7**, 11678–11685.
96 Q. Y. Liu, H. Li, Q. R. Zhao, R. R. Zhu, Y. T. Yang, Q. Y. Jia, B. Bian and L. H. Zhuo, *Mater. Sci. Eng., C*, 2014, **41**, 142–151.
97 Q. Y. Liu, Q. Y. Jia, R. R. Zhu, Q. Shao, D. M. Wang, P. Cui and J. C. Ge, *Mater. Sci. Eng., C*, 2014, **42**, 177–184.
98 Y. X. Chen, H. H. Zhang, H. G. Xue, X. Y. Hu, G. X. Wang and C. Y. Wang, *Mater. Sci. Eng., C*, 2014, **35**, 420–425.
99 B. Liu, Z. Sun, P.-J. J. Huang and J. Liu, *J. Am. Chem. Soc.*, 2015, **137**, 1290–1295.
100 H. Wang, S. Li, Y. M. Si, Z. Z. Sun, S. Y. Li and Y. H. Lin, *J. Mater. Chem. B*, 2014, **2**, 4442–4448.
101 N. J. Lang, B. W. Liu and J. W. Liu, *J. Colloid Interface Sci.*, 2014, **428**, 78–83.
102 L. Li, C. Zeng, L. Ai and J. Jiang, *J. Alloys Compd.*, 2015, **639**, 470–477.
103 T. Tian, L. H. Ai, X. M. Liu, L. L. Li, J. Li and J. Jiang, *Ind. Eng. Chem. Res.*, 2015, **54**, 1171–1178.
104 K. G. Qu, P. Shi, J. S. Ren and X. G. Qu, *Chem. – Eur. J.*, 2014, **20**, 7501–7506.
105 L. J. Wan, J. H. Liu and X. J. Huang, *Chem. Commun.*, 2014, **50**, 13589–13591.
106 Y. J. Chen, H. Y. Cao, W. B. Shi, H. Liu and Y. M. Huang, *Chem. Commun.*, 2013, **49**, 5013–5015.
107 Z. C. Xing, J. Q. Tian, A. M. Asiri, A. H. Qusti, A. O. Al-Youbi and X. P. Sun, *Biosens. Bioelectron.*, 2014, **52**, 452–457.
108 L. Su, W. J. Qin, H. G. Zhang, Z. U. Rahman, C. L. Ren, S. D. Ma and X. G. Chen, *Biosens. Bioelectron.*, 2015, **63**, 384–391.
109 Y. Liu, M. Yuan, L. J. Qiao and R. Guo, *Biosens. Bioelectron.*, 2014, **52**, 391–396.
110 T. R. Lin, L. S. Zhong, J. Wang, L. Q. Guo, H. Y. Wu, Q. Q. Guo, F. F. Fu and G. N. Chen, *Biosens. Bioelectron.*, 2014, **59**, 89–93.

111 T. R. Lin, L. S. Zhong, Z. P. Song, L. Q. Guo, H. Y. Wu, Q. Q. Guo, Y. Chen, F. F. Fu and G. N. Chen, *Biosens. Bioelectron.*, 2014, **62**, 302–307.
112 R. M. Li, M. M. Zhen, M. R. Guan, D. Q. Chen, G. Q. Zhang, J. C. Ge, P. Gong, C. R. Wang and C. Y. Shu, *Biosens. Bioelectron.*, 2013, **47**, 502–507.
113 K. Mitra, A. B. Ghosh, A. Sarkar, N. Saha and A. K. Dutta, *Biochem. Biophys. Res. Commun.*, 2014, **451**, 30–35.
114 J. X. Xie, H. Y. Cao, H. Jiang, Y. J. Chen, W. B. Shi, H. Z. Zheng and Y. M. Huang, *Anal. Chim. Acta*, 2013, **796**, 92–100.
115 S. Zhu, X.-E. Zhao, J. You, G. Xu and H. Wang, *Analyst*, 2015, **140**, 6398–6403.
116 Y. L. Liu, X. J. Zhao, X. X. Yang and Y. F. Li, *Analyst*, 2013, **138**, 4526–4531.
117 Y. Guo, W. W. Li, M. Y. Zheng and Y. Huang, *Acta Chim. Sin.*, 2014, **72**, 713–719.
118 R. Qu, L. L. Shen, A. T. Qu, R. L. Wang, Y. L. An and L. Q. Shi, *ACS Appl. Mater. Interfaces*, 2015, **7**, 16694–16705.
119 C. Lu, X. J. Liu, Y. F. Li, F. Yu, L. H. Tang, Y. J. Hu and Y. B. Yine, *ACS Appl. Mater. Interfaces*, 2015, **7**, 15395–15402.
120 L. Han, C. C. Li, T. Zhang, Q. L. Lang and A. H. Liu, *ACS Appl. Mater. Interfaces*, 2015, **7**, 14463–14470.
121 L. Su, J. Feng, X. M. Zhou, C. L. Ren, H. H. Li and X. G. Chen, *Anal. Chem.*, 2012, **84**, 5753–5758.
122 W. Haider, A. Hayat, Y. Raza, A. A. Chaudhry, R. Ihtesham Ur and J. L. Marty, *RSC Adv.*, 2015, **5**, 24853–24858.
123 S. B. He, G. W. Wu, H. H. Deng, A. L. Liu, X. H. Lin, X. H. Xia and W. Chen, *Biosens. Bioelectron.*, 2014, **62**, 331–336.
124 Y. R. Tang, Y. Zhang, R. Liu, Y. Y. Su and Y. Lu, *Chin. J. Anal. Chem.*, 2013, **41**, 330–336.
125 C. I. Wang, W. T. Chen and H. T. Chang, *Anal. Chem.*, 2012, **84**, 9706–9712.
126 M. M. Liang, K. L. Fan, Y. Pan, H. Jiang, F. Wang, D. L. Yang, D. Lu, J. Feng, J. J. Zhao, L. Yang and X. Y. Yan, *Anal. Chem.*, 2013, **85**, 308–312.
127 J. Qian, X. W. Yang, L. Jiang, C. D. Zhu, H. P. Mao and K. Wang, *Sens. Actuators, B*, 2014, **201**, 160–166.
128 M. Shamsipur, A. Safavi and Z. Mohammadpour, *Sens. Actuators, B*, 2014, **199**, 463–469.
129 P. J. Ni, H. C. Dai, Y. L. Wang, Y. J. Sun, Y. Shi, J. T. Hu and Z. Li, *Biosens. Bioelectron.*, 2014, **60**, 286–291.
130 X. Y. Niu, Y. Y. Xu, Y. L. Dong, L. Y. Qi, S. D. Qi, H. L. Chen and X. G. Chen, *J. Alloys Compd.*, 2014, **587**, 74–81.
131 H. L. Tan, C. J. Ma, L. Gao, Q. Li, Y. H. Song, F. G. Xu, T. Wang and L. Wang, *Chem. – Eur. J.*, 2014, **20**, 16377–16383.
132 Y. Ma, C. Yu and X. Chen, *J. Anal. Sci.*, 2014, **30**, 709–712.
133 J. R. Li, G. N. Zhang, L. H. Wang, A. G. Shen and J. M. Hu, *Talanta*, 2015, **140**, 204–211.
134 Y. Sun, J. Wang, W. Li, J. Zhang, Y. Zhang and Y. Fu, *Biosens. Bioelectron.*, 2015, **74**, 1038–1046.
135 X. Q. Lin, H. H. Deng, G. W. Wu, H. P. Peng, A. L. Liu, X. H. Lin, X. H. Xia and W. Chen, *Analyst*, 2015, **140**, 5251–5256.
136 D. Y. Zhang, Z. Chen, H. Omar, L. Deng and N. M. Khashab, *ACS Appl. Mater. Interfaces*, 2015, **7**, 4589–4594.
137 C. X. Chen, L. X. Lu, Y. Zheng, D. Zhao, F. Yang and X. R. Yang, *Anal. Methods*, 2015, **7**, 161–167.
138 G. L. Wang, L. Y. Jin, Y. M. Dong, X. M. Wu and Z. J. Li, *Biosens. Bioelectron.*, 2015, **64**, 523–529.
139 H. Cheng, X. Wang and H. Wei, *Anal. Chem.*, 2015, **87**, 8889–8895.
140 G. J. Guan, L. Yang, Q. S. Mei, K. Zhang, Z. P. Zhang and M. Y. Han, *Anal. Chem.*, 2012, **84**, 9492–9497.
141 X. D. Zhang, S. H. He, Z. H. Chen and Y. M. Huang, *J. Agric. Food Chem.*, 2013, **61**, 840–847.
142 W. J. Qin, L. Su, C. Yang, Y. H. Ma, H. J. Zhang and X. G. Chen, *J. Agric. Food Chem.*, 2014, **62**, 5827–5834.
143 A. Hayat, J. Cunningham, G. Bulbul and S. Andreescu, *Anal. Chim. Acta*, 2015, **885**, 140–147.
144 Y. H. Xiong, S. H. Chen, F. G. Ye, L. J. Su, C. Zhang, S. F. Shen and S. L. Zhao, *Chem. Commun.*, 2015, **51**, 4635–4638.
145 Y. J. Guo, L. Deng, J. Li, S. J. Guo, E. K. Wang and S. J. Dong, *ACS Nano*, 2011, **5**, 1282–1290.
146 Q. B. Wang, J. P. Lei, S. Y. Deng, L. Zhang and H. X. Ju, *Chem. Commun.*, 2013, **49**, 916–918.
147 R. Thiramanas, K. Jangpatarapongsa, P. Tangboriboonrat and D. Polpanich, *Anal. Chem.*, 2013, **85**, 5996–6002.
148 M. I. Kim, K. S. Park and H. G. Park, *Chem. Commun.*, 2014, **50**, 9577–9580.
149 G. F. Wang, L. Chen, X. P. He, Y. H. Zhu and X. J. Zhang, *Analyst*, 2014, **139**, 3895–3900.
150 Z. F. Wang, X. Yang, J. Feng, Y. J. Tang, Y. Y. Jiang and N. Y. He, *Analyst*, 2014, **139**, 6088–6091.
151 S. Y. Deng, P. X. Yuan, X. B. Ji, D. Shan and X. J. Zhang, *ACS Appl. Mater. Interfaces*, 2015, **7**, 543–552.
152 G. L. Wang, K. L. Liu, J. X. Shu, T. T. Gu, X. M. Wu, Y. M. Dong and Z. J. Li, *Biosens. Bioelectron.*, 2015, **69**, 106–112.
153 G. Y. Zhang, S. Y. Deng, W. R. Cai, S. Cosnier, X. J. Zhang and D. Shan, *Anal. Chem.*, 2015, **87**, 9093–9100.
154 G. L. Wang, L. Y. Jin, X. M. Wu, Y. M. Dong and Z. J. Li, *Anal. Chim. Acta*, 2015, **871**, 1–8.
155 Y. Song, Y. Wang and L. Qin, *J. Am. Chem. Soc.*, 2013, **135**, 16785–16788.
156 M. Liu, H. M. Zhao, S. Chen, H. T. Yu and X. Quan, *Chem. Commun.*, 2012, **48**, 7055–7057.
157 B. Zou, Y. Liu, J. Wang and C. Huang, *Sci. Sin. Chim.*, 2014, **44**, 1641–1646.
158 B. W. Liu and J. W. Liu, *Nanoscale*, 2015, **7**, 13831–13835.
159 P. Weerathunge, R. Ramanathan, R. Shukla, T. K. Sharma and V. Bansal, *Anal. Chem.*, 2014, **86**, 11937–11941.
160 Y. S. Kim and J. Jurng, *Sens. Actuators, B*, 2013, **176**, 253–257.

161 R. Pautler, E. Y. Kelly, P. J. J. Huang, J. Cao, B. W. Liu and J. W. Liu, *ACS Appl. Mater. Interfaces*, 2013, **5**, 6820–6825.
162 L. C. Bock, L. C. Griffin, J. A. Latham, E. H. Vermaas and J. J. Toole, *Nature*, 1992, **355**, 564–566.
163 T. Hermann and D. J. Patel, *Science*, 2000, **287**, 820–825.
164 J. W. Liu, Z. H. Cao and Y. Lu, *Chem. Rev.*, 2009, **109**, 1948–1998.
165 H. Wei, B. L. Li, J. Li, E. K. Wang and S. J. Dong, *Chem. Commun.*, 2007, 3735–3737.
166 Y. Wang, H. Wei, B. Li, W. Ren, S. Guo, S. Dong and E. Wang, *Chem. Commun.*, 2007, 5220–5222.
167 B. L. Li, H. Wei and S. J. Dong, *Chem. Commun.*, 2007, 73–75.
168 Y. Du, B. L. Li, H. Wei, Y. L. Wang and E. K. Wang, *Anal. Chem.*, 2008, **80**, 5110–5117.
169 B. L. Li, Y. L. Wang, H. Wei and S. J. Dong, *Biosens. Bioelectron.*, 2008, **23**, 965–970.
170 L. Y. Fang, Z. Z. Lv, H. Wei and E. Wang, *Anal. Chim. Acta*, 2008, **628**, 80–86.
171 B. L. Li, Y. Du, H. Wei and S. J. Dong, *Chem. Commun.*, 2007, 3780–3782.
172 L. B. Zhang, H. Wei, J. Li, T. Li, D. Li, Y. H. Li and E. K. Wang, *Biosens. Bioelectron.*, 2010, **25**, 1897–1901.
173 J. G. Bai, H. Wei, B. L. Li, L. H. Song, L. Y. Fang, Z. Z. Lv, W. H. Zhou and E. K. Wang, *Chem. – Asian J.*, 2008, **3**, 1935–1941.
174 L. Y. Fang, Z. Z. Lu, H. Wei and E. K. Wang, *Biosens. Bioelectron.*, 2008, **23**, 1645–1651.
175 B. Wang, C. L. Guo, G. J. Chen, B. Park and B. Q. Xu, *Chem. Commun.*, 2012, **48**, 1644–1646.
176 B. Wang, C. L. Guo, M. M. Zhang, B. Park and B. Q. Xu, *J. Phys. Chem. B*, 2012, **116**, 5316–5322.
177 S. Y. Zhang, Y. B. Ding and H. Wei, *Molecules*, 2014, **19**, 11933–11987.
178 T. K. Sharma, R. Ramanathan, P. Weerathunge, M. Mohammadtaheri, H. K. Daima, R. Shukla and V. Bansal, *Chem. Commun.*, 2014, **50**, 15856–15859.
179 P. Jing, W. J. Xu, H. Y. Yi, Y. M. Wu, L. J. Bai and R. Yuan, *Analyst*, 2014, **139**, 1756–1761.
180 W. J. Xu, S. Y. Xue, H. Y. Yi, P. Jing, Y. Q. Chai and R. Yuan, *Chem. Commun.*, 2015, **51**, 1472–1474.
181 C. Zheng, A. X. Zheng, B. Liu, X. L. Zhang, Y. He, J. Li, H. H. Yang and G. N. Chen, *Chem. Commun.*, 2014, **50**, 13103–13106.
182 L. Chen, L. Sha, Y. W. Qiu, G. F. Wang, H. Jiang and X. J. Zhang, *Nanoscale*, 2015, **7**, 3300–3308.
183 S. M. Taghdisi, N. M. Danesh, P. Lavaee, A. S. Emrani, M. Ramezani and K. Abnous, *RSC Adv.*, 2015, **5**, 43508–43514.
184 H. Wei, B. L. Li, J. Li, S. J. Dong and E. K. Wang, *Nanotechnology*, 2008, **19**, 095501.
185 Y. Song, K. Qu, C. Xu, J. Ren and X. Qu, *Chem. Commun.*, 2010, **46**, 6572–6574.
186 R. Zhu, Y. Zhou, X. L. Wang, L. P. Liang, Y. J. Long, Q. L. Wang, H. J. Zhang, X. X. Huang and H. Z. Zheng, *Talanta*, 2013, **117**, 127–132.
187 C.-W. Lien, Y.-C. Chen, H.-T. Chang and C.-C. Huang, *Nanoscale*, 2013, **5**, 8227–8234.
188 Y. S. Wu, F. F. Huang and Y. W. Lin, *ACS Appl. Mater. Interfaces*, 2013, **5**, 1503–1509.
189 C.-W. Lien, Y.-T. Tseng, C.-C. Huang and H.-T. Chang, *Anal. Chem.*, 2014, **86**, 2065–2072.
190 Z. Mohammadpour, A. Safavi and M. Shamsipur, *Chem. Eng. J.*, 2014, **255**, 1–7.
191 Y. Fu, H. X. Zhang, S. D. Dai, X. Zhi, J. L. Zhang and W. Li, *Analyst*, 2015, **140**, 6676–6683.
192 H. Abdolmohammad-Zadeh and E. Rahimpour, *Sens. Actuators, B*, 2015, **209**, 496–504.
193 W. Li, B. Chen, H. Zhang, Y. Sun, J. Wang, J. Zhang and Y. Fu, *Biosens. Bioelectron.*, 2015, **66**, 251–258.
194 H. G. Yang, Y. H. Xiong, P. Zhang, L. J. Su and F. G. Ye, *Anal. Methods*, 2015, **7**, 4596–4601.
195 W. Li, H. X. Zhang, J. L. Zhang and Y. Fu, *Anal. Methods*, 2015, **7**, 4464–4471.
196 G. W. Wu, S. B. He, H. P. Peng, H. H. Deng, A. L. Liu, X. H. Lin, X. H. Xia and W. Chen, *Anal. Chem.*, 2014, **86**, 10955–10960.
197 Z. Q. Gao, M. D. Xu, L. Hou, G. N. Chen and D. P. Tang, *Anal. Chem.*, 2013, **85**, 6945–6952.
198 Y. C. Lee, M. I. Kim, M. A. Woo, H. G. Park and J. I. Han, *Biosens. Bioelectron.*, 2013, **42**, 373–378.
199 Z. F. Wang, S. Zheng, J. Cai, P. Wang, J. Feng, X. Yang, L. M. Zhang, M. Ji, F. G. Wu, N. Y. He and N. Wan, *Anal. Chem.*, 2013, **85**, 11602–11609.
200 J. L. Dong, L. N. Song, J. J. Yin, W. W. He, Y. H. Wu, N. Gu and Y. Zhang, *ACS Appl. Mater. Interfaces*, 2014, **6**, 1959–1970.
201 Z. H. Yang, Y. Q. Chai, R. Yuan, Y. Zhuo, Y. Li, J. Han and N. Liao, *Sens. Actuators, B*, 2014, **193**, 461–466.
202 J. L. Wen, S. G. Zhou and J. H. Chen, *Sci. Rep.*, 2014, **4**, 5191.
203 X. N. Hu, A. Saran, S. Hou, T. Wen, Y. L. Ji, W. Q. Liu, H. Zhang and X. C. Wu, *Chin. Sci. Bull.*, 2014, **59**, 2588–2596.
204 L. Zhan, C. M. Li, W. B. Wu and C. Z. Huang, *Chem. Commun.*, 2014, **50**, 11526–11528.
205 G. L. Wang, X. F. Xu, L. Qiu, Y. M. Dong, Z. J. Li and C. Zhang, *ACS Appl. Mater. Interfaces*, 2014, **6**, 6434–6442.
206 M. I. Kim, Y. Ye, M. A. Woo, J. Lee and H. G. Park, *Adv. Healthcare Mater.*, 2014, **3**, 36–41.
207 Y. Song, X. Xia, X. Wu, P. Wang and L. Qin, *Angew. Chem., Int. Ed.*, 2014, **53**, 12451–12455.
208 Y. Cai, C. Q. Cao, X. Q. He, C. Y. Yang, L. X. Tian, R. X. Zhu and Y. X. Pan, *Int. J. Nanomed.*, 2015, **10**, 2619–2634.
209 S. K. Maji, A. K. Mandal, K. T. Nguyen, P. Borah and Y. L. Zhao, *ACS Appl. Mater. Interfaces*, 2015, **7**, 9807–9816.
210 Z. Gao, M. Xu, M. Lu, G. Chen and D. Tang, *Biosens. Bioelectron.*, 2015, **70**, 194–201.
211 D. Duan, K. Fan, D. Zhang, S. Tan, M. Liang, Y. Liu, J. Zhang, P. Zhang, W. Liu, X. Qiu, G. P. Kobinger,

G. F. Gao and X. Yan, *Biosens. Bioelectron.*, 2015, **74**, 134–141.
212 Z. Tian, J. Li, Z. Zhang, W. Gao, X. Zhou and Y. Qu, *Biomaterials*, 2015, **59**, 116–124.
213 M. Kim, M. S. Kim, S. H. Kweon, S. Jeong, M. H. Kang, M. I. Kim, J. Lee and J. Doh, *Adv. Healthcare Mater.*, 2015, **4**, 1311–1316.
214 J. Shu, Z. Qiu, Q. Wei, J. Zhuang and D. Tang, *Sci. Rep.*, 2015, **5**, 15113.
215 Y. Li, J. Xuan, Y. Song, P. Wang and L. Qin, *Lab Chip*, 2015, **15**, 3300–3306.
216 Z. Zhu, Z. Guan, S. Jia, Z. Lei, S. Lin, H. Zhang, Y. Ma, Z.-Q. Tian and C. J. Yang, *Angew. Chem., Int. Ed.*, 2014, **53**, 12503–12507.
217 A. Asati, C. Kaittanis, S. Santra and J. M. Perez, *Anal. Chem.*, 2011, **83**, 2547–2553.
218 Y. Tao, Y. H. Lin, Z. Z. Huang, J. S. Ren and X. G. Qu, *Adv. Mater.*, 2013, **25**, 2594–2599.
219 Z. J. Zhang, Y. J. Guan, M. Li, A. D. Zhao, J. S. Ren and X. G. Qu, *Chem. Sci.*, 2015, **6**, 2822–2826.
220 L. N. Zhang, H. H. Deng, F. L. Lin, X. W. Xu, S. H. Weng, A. L. Liu, X. H. Lin, X. H. Xia and W. Chen, *Anal. Chem.*, 2014, **86**, 2711–2718.
221 K. Fan, C. Cao, Y. Pan, D. Lu, D. Yang, J. Feng, L. Song, M. Liang and X. Yan, *Nat. Nanotechnol.*, 2012, **7**, 459–464.
222 S. S. Ali, J. I. Hardt, K. L. Quick, J. S. Kim-Han, B. F. Erlanger, T. T. Huang, C. J. Epstein and L. L. Dugan, *Free Radicals Biol. Med.*, 2004, **37**, 1191–1202.
223 S. S. Ali, J. I. Hardt and L. L. Dugan, *Nanomed. Nanotechnol. Biol. Med.*, 2008, **4**, 283–294.
224 K. L. Quick, S. S. Ali, R. Arch, C. Xiong, D. Wozniak and L. L. Dugan, *Neurobiol. Aging*, 2008, **29**, 117–128.
225 D. M. Huang, J. K. Hsiao, Y. C. Chen, L. Y. Chien, M. Yao, Y. K. Chen, B. S. Ko, S. C. Hsu, L. A. Tai, H. Y. Cheng, S. W. Wang, C. S. Yang and Y. C. Chen, *Biomaterials*, 2009, **30**, 3645–3651.
226 C. Mandoli, F. Pagliari, S. Pagliari, G. Forte, P. Di Nardo, S. Licoccia and E. Traversa, *Adv. Funct. Mater.*, 2010, **20**, 1617–1624.
227 C. K. Kim, T. Kim, I.-Y. Choi, M. Soh, D. Kim, Y.-J. Kim, H. Jang, H.-S. Yang, J. Y. Kim, H.-K. Park, S. P. Park, S. Park, T. Yu, B.-W. Yoon, S.-H. Lee and T. Hyeon, *Angew. Chem., Int. Ed.*, 2012, **51**, 11039–11043.
228 T. Kito, R. Shibata, M. Ishii, H. Suzuki, T. Himeno, Y. Kataoka, Y. Yamamura, T. Yamamoto, N. Nishio, S. Ito, Y. Numaguchi, T. Tanigawa, J. K. Yamashita, N. Ouchi, H. Honda, K. Isobe and T. Murohara, *Sci. Rep.*, 2013, **3**, 1418.
229 R. Ragg, F. Natalio, M. N. Tahir, H. Janssen, A. Kashyap, D. Strand, S. Strand and W. Tremel, *ACS Nano*, 2014, **8**, 5182–5189.
230 J. M. Dowding, W. Song, K. Bossy, A. Karakoti, A. Kumar, A. Kim, B. Bossy, S. Seal, M. H. Ellisman, G. Perkins, W. T. Self and E. Bossy-Wetzel, *Cell Death Differ.*, 2014, **21**, 1622–1632.
231 L. Z. Gao, K. M. Giglio, J. L. Nelson, H. Sondermann and A. J. Travis, *Nanoscale*, 2014, **6**, 2588–2593.
232 D. Son, J. Lee, D. J. Lee, R. Ghaffari, S. Yun, S. J. Kim, J. E. Lee, H. R. Cho, S. Yoon, S. Yang, S. Lee, S. Qiao, D. Ling, S. Shin, J.-K. Song, J. Kim, T. Kim, H. Lee, J. Kim, M. Soh, N. Lee, C. S. Hwang, S. Nam, N. Lu, T. Hyeon, S. H. Choi and D.-H. Kim, *ACS Nano*, 2015, **9**, 5937–5946.
233 M. J. Akhtar, M. Ahamed, H. A. Alhadlaq, M. A. M. Khan and S. A. Alrokayan, *J. Colloid Interface Sci.*, 2015, **453**, 21–27.
234 H. Su, D. D. Liu, M. Zhao, W. L. Hu, S. S. Xue, Q. Cao, X. Y. Le, L. N. Ji and Z. W. Mao, *ACS Appl. Mater. Interfaces*, 2015, **7**, 8233–8242.
235 M. J. Akhtar, M. Ahamed, H. A. Alhadlaq, A. Alshamsan, M. A. M. Khan and S. A. Alrokayan, *J. Colloid Interface Sci.*, 2015, **457**, 370–377.
236 A. B. Shcherbakov, N. M. Zholobak, A. E. Baranchikov, A. V. Ryabova and V. K. Ivanov, *Mater. Sci. Eng., C*, 2015, **50**, 151–159.
237 D.-M. Huang, J.-K. Hsiao, Y.-C. Chen, L.-Y. Chien, M. Yao, Y.-K. Chen, B.-S. Ko, S.-C. Hsu, L.-A. Tai, H.-Y. Cheng, S.-W. Wang, C.-S. Yang and Y.-C. Chen, *Biomaterials*, 2009, **30**, 3645–3651.
238 H. J. Cheng and H. Wei, Gordon Research Conference: Bioanalytical Sensors, Newport, RI, USA, June 22–27, 2014.
239 M. Mittal, M. R. Siddiqui, K. Tran, S. P. Reddy and A. B. Malik, *Antioxid. Redox Signaling*, 2014, **20**, 1126–1167.
240 S. M. Hirst, A. S. Karakoti, R. D. Tyler, N. Sriranganathan, S. Seal and C. M. Reilly, *Small*, 2009, **5**, 2848–2856.
241 F. Pagliari, C. Mandoli, G. Forte, E. Magnani, S. Pagliari, G. Nardone, S. Licoccia, M. Minieri, P. Di Nardo and E. Traversa, *ACS Nano*, 2012, **6**, 3767–3775.
242 F. Natalio, R. Andre, A. F. Hartog, B. Stoll, K. P. Jochum, R. Wever and W. Tremel, *Nat. Nanotechnol.*, 2012, **7**, 530–535.
243 T. Xue, B. Peng, M. Xue, X. Zhong, C.-Y. Chiu, S. Yang, Y. Qu, L. Ruan, S. Jiang, S. Dubin, R. B. Kaner, J. I. Zink, M. E. Meyerhoff, X. Duan and Y. Huang, *Nat. Commun.*, 2014, **5**, 3200.
244 R. Andre, F. Natalio, M. Humanes, J. Leppin, K. Heinze, R. Wever, H. C. Schroeder, W. E. G. Mueller and W. Tremel, *Adv. Funct. Mater.*, 2011, **21**, 501–509.
245 J. Zhuang, K. L. Fan, L. Z. Gao, D. Lu, J. Feng, D. L. Yang, N. Gu, Y. Zhang, M. M. Liang and X. Y. Yan, *Mol. Pharm.*, 2012, **9**, 1983–1989.
246 F. Xiong, H. Wang, Y. D. Feng, Y. M. Li, X. Q. Hua, X. Y. Pang, S. Zhang, L. Song, Y. Zhang and N. Gu, *Sci. Rep.*, 2015, **5**, 8579.
247 Z. Liu, X. Liu, Y. Du, J. Ren and X. Qu, *ACS Nano*, 2015, **9**, 10335–10346.
248 Y. Lin, C. Xu, J. Ren and X. Qu, *Angew. Chem., Int. Ed.*, 2012, **51**, 12579–12583.
249 B. Lin, Q. Q. Sun, K. Liu, D. Q. Lu, Y. Fu, Z. A. Xu and W. Zhang, *Langmuir*, 2014, **30**, 2144–2151.

250 J. Zhang, J. Zhuang, L. Gao, Y. Zhang, N. Gu, J. Feng, D. Yang, J. Zhu and X. Yan, *Chemosphere*, 2008, **73**, 1524–1528.
251 Q. Cai, S. K. Lu, F. Liao, Y. Q. Li, S. Z. Ma and M. W. Shao, *Nanoscale*, 2014, **6**, 8117–8123.
252 X. C. Wu, Y. Zhang, T. Han, H. X. Wu, S. W. Guo and J. Y. Zhang, *RSC Adv.*, 2014, **4**, 3299–3305.
253 H. Y. Chang, J. S. Cang, P. Roy, H. T. Chang, Y. C. Huang and C. C. Huang, *ACS Appl. Mater. Interfaces*, 2014, **6**, 8305–8312.
254 Z. Liu, X. Liu, X. Ran, E. Ju, J. Ren and X. Qu, *Biomaterials*, 2015, **69**, 56–64.
255 P. F. Zhan, Z. G. Wang, N. Li and B. Q. Ding, *ACS Catal.*, 2015, **5**, 1489–1498.
256 C. Korsvik, S. Patil, S. Seal and W. T. Self, *Chem. Commun.*, 2007, 1056–1058.
257 Z. Y. Yang, S. L. Luo, H. Li, S. W. Dong, J. He, H. Jiang, R. Li and X. C. Yang, *RSC Adv.*, 2014, **4**, 59965–59969.
258 Y. Fu, X. Y. Zhao, J. L. Zhang and W. Li, *J. Phys. Chem. C*, 2014, **118**, 18116–18125.
259 Y. Liu, H. Wu, Y. Chong, W. G. Wamer, Q. Xia, L. Cai, Z. Nie, P. P. Fu and J.-J. Yin, *ACS Appl. Mater. Interfaces*, 2015, **7**, 19709–19717.
260 Y. L. Guo, X. Y. Liu, C. D. Yang, X. D. Wang, D. Wang, A. Iqbal, W. S. Liu and W. W. Qin, *ChemCatChem*, 2015, **7**, 2467–2474.
261 W. Shi, X. Zhang, S. He, J. Li and Y. Huang, *Sci. Sin. Chim.*, 2013, **43**, 1591–1598.
262 J. Xu, J. Wu, C. Zong, H. X. Ju and F. Yan, *Anal. Chem.*, 2013, **85**, 3374–3379.
263 Z. Y. Can, A. Uzer, K. Turkekul, E. Ercag and R. Apak, *Anal. Chem.*, 2015, **87**, 9589–9594.
264 B. Reuillard, S. Gentil, M. Carriere, A. Le Goff and S. Cosnier, *Chem. Sci.*, 2015, **6**, 5139–5143.
265 Y. Tao, E. G. Ju, J. S. Ren and X. G. Qu, *Adv. Mater.*, 2015, **27**, 1097–1104.
266 R. Cai, D. Yang, S. Peng, X. Chen, Y. Huang, Y. Liu, W. Hou, S. Yang, Z. Liu and W. Tan, *J. Am. Chem. Soc.*, 2015, **137**, 13957–13963.
267 Y. Liu, D. L. Purich, C. Wu, Y. Wu, T. Chen, C. Cui, L. Zhang, S. Cansiz, W. Hou, Y. Wang, S. Yang and W. Tan, *J. Am. Chem. Soc.*, 2015, **137**, 14952–14958.
268 Y. Lu, N. Yeung, N. Sieracki and N. M. Marshall, *Nature*, 2009, **460**, 855–862.
269 I. Samish, C. M. MacDermaid, J. M. Perez-Aguilar and J. G. Saven, *Annu. Rev. Phys. Chem.*, 2011, **62**, 129–149.
270 J. X. Xie, X. D. Zhang, H. Jiang, S. Wang, H. Liu and Y. M. Huang, *RSC Adv.*, 2014, **4**, 26046–26049.
271 X. Ai, Y. Wang, X. D. Hou, L. Yang, C. B. Zheng and L. Wu, *Analyst*, 2013, **138**, 3494–3501.
272 S. Saraf, C. J. Neal, S. Das, S. Barkam, R. McCormack and S. Seal, *ACS Appl. Mater. Interfaces*, 2014, **6**, 5472–5482.
273 H. Sun, A. Zhao, N. Gao, K. Li, J. Ren and X. Qu, *Angew. Chem., Int. Ed.*, 2015, **54**, 7176–7180.
274 Y. Li, X. He, J.-J. Yin, Y. Ma, P. Zhang, J. Li, Y. Ding, J. Zhang, Y. Zhao, Z. Chai and Z. Zhang, *Angew. Chem., Int. Ed.*, 2015, **54**, 1832–1835.
275 X. F. Lu, X. J. Bian, Z. C. Li, D. M. Chao and C. Wang, *Sci. Rep.*, 2013, **3**, 2955.
276 Y. H. Lin, L. Wu, Y. Y. Huang, J. S. Ren and X. G. Qu, *Chem. Sci.*, 2015, **6**, 1272–1276.
277 Y. Y. Huang, X. Ran, Y. H. Lin, J. S. Ren and X. G. Qu, *Chem. Commun.*, 2015, **51**, 4386–4389.
278 X. N. Hu, A. Saran, S. Hou, T. Wen, Y. L. Ji, W. Q. Liu, H. Zhang, W. W. He, J. J. Yin and X. C. Wu, *RSC Adv.*, 2013, **3**, 6095–6105.
279 U. Carmona, L. B. Zhang, L. Li, W. Munchgesang, E. Pippel and M. Knez, *Chem. Commun.*, 2014, **50**, 701–703.
280 Y. W. Fan, W. B. Shi, X. D. Zhang and Y. M. Huang, *J. Mater. Chem. A*, 2014, **2**, 2482–2486.
281 L. L. Li, L. H. Ai, C. H. Zhang and J. Jiang, *Nanoscale*, 2014, **6**, 4627–4634.
282 Y. H. Lin, A. D. Zhao, Y. Tao, J. S. Ren and X. G. Qu, *J. Am. Chem. Soc.*, 2013, **135**, 4207–4210.
283 J. Li, W. Liu, X. Wu and X. Gao, *Biomaterials*, 2015, **48**, 37–44.
284 W. P. R. Deleu, G. Rivero, R. F. A. Teixeira, F. E. Du Prez and D. E. De Vos, *Chem. Mater.*, 2015, **27**, 5495–5502.
285 G. Y. Tonga, Y. D. Jeong, B. Duncan, T. Mizuhara, R. Mout, R. Das, S. T. Kim, Y. C. Yeh, B. Yan, S. Hou and V. M. Rotello, *Nat. Chem.*, 2015, **7**, 597–603.
286 H. Wei, Z. D. Wang, J. Zhang, S. House, Y. G. Gao, L. M. Yang, H. Robinson, L. H. Tan, H. Xing, C. J. Hou, I. M. Robertson, J. M. Zuo and Y. Lu, *Nat. Nanotechnol.*, 2011, **6**, 93–97.
287 H. Wei and Y. Lu, *Chem. – Asian J.*, 2012, **7**, 680–683.
288 H. Wei, S. House, J. J. X. Wu, J. Zhang, Z. D. Wang, Y. He, E. J. Gao, Y. G. Gao, H. Robinson, W. Li, J. M. Zuo, I. M. Robertson and Y. Lu, *Nano Res.*, 2013, **6**, 627–634.
289 Y. B. Ding, L. L. Shi and H. Wei, *J. Mater. Chem. B*, 2014, **2**, 8268–8291.
290 Y. H. Hu, W. J. Guo and H. Wei, *Isr. J. Chem.*, 2015, **55**, 682–697.

